

Bayesian Kernel Two-Sample Testing

Qinyi Zhang

Department of Statistics, University of Oxford

Sarah Filippi

Department of Mathematics, Imperial College London

Seth Flaxman

Department of Mathematics, Imperial College London

Dino Sejdinovic

Department of Statistics, University of Oxford

March 23, 2022

Abstract

In modern data analysis, nonparametric measures of discrepancies between random variables are particularly important. The subject is well-studied in the frequentist literature, while the development in the Bayesian setting is limited where applications are often restricted to univariate cases. Here, we propose a Bayesian kernel two-sample testing procedure based on modelling the difference between kernel mean embeddings in the reproducing kernel Hilbert space utilising the framework established by Flaxman et al. [2016]. The use of kernel methods enables its application to random variables in generic domains beyond the multivariate Euclidean spaces. The proposed procedure results in a posterior inference scheme that allows an automatic selection of the kernel parameters relevant to the problem at hand. In a series of synthetic experiments and two real data experiments (i.e. testing network heterogeneity from high-dimensional data and six-membered monocyclic ring conformation comparison), we illustrate the advantages of our approach.

Keywords: Hypothesis testing, dependence measure, kernel mean embeddings, Bayes factor

1 Introduction

Nonparametric two-sample testing is an important branch of hypothesis testing with a wide range of applications. The two-sample testing problem can be described as follows: given a set of samples $\{x_i\}_{i=1}^{n_x} \stackrel{i.i.d.}{\sim} P$ and $\{y_i\}_{i=1}^{n_y} \stackrel{i.i.d.}{\sim} Q$, we wish to evaluate the evidence for the competing hypotheses

$$H_0 : P = Q \text{ v.s. } H_1 : P \neq Q \quad (1)$$

with the probability distributions P and Q unknown. In this work, we will pursue a Bayesian perspective to this problem. In this perspective, hypotheses can be formulated as models and hypothesis testing can therefore be viewed as a form of model selection, i.e. to identify which model is strongly supported by the data [Jeffreys and Berger, 1992].

The classical Bayesian formulation of the two-sample testing problem is in terms of the Bayes factor [Jeffreys, 1935, 1961, Kass and Raftery, 1995]. For a given data set \mathcal{D} and two competing models/hypotheses M_0 (or H_0) and M_1 (or H_1) parameterised by the vectors θ_0 and θ_1 respectively, the Bayes factor is represented as the likelihood ratio of the samples given that they were generated from the same distribution (null hypothesis) to that they were generated from different distributions (alternative hypothesis):

$$BF = \frac{P(\mathcal{D}|M_0)}{P(\mathcal{D}|M_1)} \quad (2)$$

$$= \frac{\int P(\theta_0|M_0)P(\mathcal{D}|\theta_0, M_0)d\theta_0}{\int P(\theta_1|M_1)P(\mathcal{D}|\theta_1, M_1)d\theta_1} \quad (3)$$

Note, in our nonparametric two-sample testing regime, θ_0 and θ_1 are the hyperparameters. The Bayes factor can be interpreted as the posterior odds on the null distribution when the prior probability on the null distribution is $\frac{1}{2}$ [Kass and Raftery, 1995]. For the two-sample testing problem, the data set under consideration is $\mathcal{D} = \{\{x_i\}_{i=1}^{n_x}, \{y_j\}_{j=1}^{n_y}\}$. Assuming X and Y are independent, under the null hypothesis H_0 , the two samples come from the same distribution parameterised by θ_0 (i.e. a distribution for the pooled samples) which we denote as $P_{x,y} = P = Q$. This implies

$$P(\mathcal{D}|\theta_0, H_0) = \prod_{i=1}^{n_x} P_{x,y}(x_i|\theta_0) \prod_{j=1}^{n_y} P_{x,y}(y_j|\theta_0). \quad (4)$$

Under the alternative hypothesis H_1 , the two samples come from different distributions P and Q parameterised respectively by the vectors $\theta_{1,1}$ and $\theta_{1,2}$. These parameter vectors are collectively defined as $\theta_1 := (\theta_{1,1}^\top, \theta_{1,2}^\top)^\top$. This implies

$$P(\mathcal{D}|\theta_1, H_1) = \prod_{i=1}^{n_x} P(x_i|\theta_{1,1}) \prod_{j=1}^{n_y} Q(y_j|\theta_{1,2}). \quad (5)$$

If the posterior probability of the model given the data is of interest, it can be easily written in terms of the Bayes factor:

$$P(M_0|\mathcal{D}) = \frac{BF}{1+BF} \quad (6)$$

$$P(M_1|\mathcal{D}) = 1 - P(M_0|\mathcal{D}) = \frac{1}{1+BF} \quad (7)$$

When the prior probabilities on the models are not equal, the posterior probability of the null model can be written as:

$$P(M_0|\mathcal{D}) = \frac{P(M_0) \int P(\theta_0|M_0)P(\mathcal{D}|\theta_0, M_0)d\theta_0}{P(M_0) \int P(\theta_0|M_0)P(\mathcal{D}|\theta_0, M_0)d\theta_0 + P(M_1) \int P(\theta_1|M_1)P(\mathcal{D}|\theta_1, M_1)d\theta_1} \quad (8)$$

$$= \frac{BF}{BF + \frac{P(M_1)}{P(M_0)}} \quad (9)$$

where $P(M_0)$ and $P(M_1)$ denote respectively the prior for models M_0 and M_1 .

As discussed by Borgwardt and Ghahramani [2009], the crucial question is to define the hypotheses/likelihood models such that the resultant Bayesian two-sample test is general and applicable to all data. Ideally, we would like the model to cover as large a class of probability distributions as possible and is also applicable to multivariate distributions and other domains. Bayesian parametric hypothesis testing, i.e. when the probability distributions P and Q are of known form, is well developed and we refer the readers to Bernardo and Smith [2000]. Most nonparametric work has been focusing on testing a parametric model versus a nonparametric one and a detailed summary has been provided by Holmes et al. [2015]. More recently, Holmes et al. [2015] proposed to use a Pólya tree prior centered on some distribution G and model the distributions of the pooled samples $P_{x,y}$ ¹ under the null and the individual distributions P and Q under the alternative as

¹Under the null hypothesis, the samples X and Y are assumed to follow the same distribution, i.e. $P = Q$. Here we denote this distribution as $P_{x,y}$.

i.i.d. draws from such Pólya tree prior. The extension to independence testing was done by Filippi and Holmes [2016]. While this approach indeed gives a flexible model of the underlying probability distributions, it can only be used for 1-dimensional data.

Borgwardt and Ghahramani [2009] proposed two Bayesian two-sample tests based on Bayes factor: a parametric test using exponential families to describe the marginal likelihood distribution for the pooled samples and the individual samples; a nonparametric test using Dirichlet process mixture models (DPMM) with exponential families. For the proposed nonparametric test, the prior on probability distributions allows the applications to multivariate data. Also utilising the Bayes factor as a model comparison tool, Stegle et al. [2010] used Gaussian processes (GP) to model the probability of the observed data under each model in the problem of testing whether a gene is differentially expressed. The values of the hyperparameters (i.e. the kernel hyperparameters and the variance of the noise distribution of the GP model) were set to those that maximise the log posterior distribution of the hyperparameters. While this approach is for detecting the genes that are differentially expressed, they proposed a mixture type of approach for detecting the intervals of the time series such that the effect is present. A binary switch variable was introduced at every observation time point to determine the model that describes the expression level at that time point. Posterior inference of such variable is achieved through variational approximation.

In the independence testing literature, Filippi et al. [2016] proposed to model the probability distributions using DPMM with Gaussian distributions for pairwise dependency detection in large multivariate datasets. Though in theory the Bayes factor with DPM on the unknown densities can be computed via the marginal likelihood, this requires integrating over infinite dimensional parameter space which results in an intractable form [Filippi et al., 2016]. Hence the problem was reformulated using a mixture modelling approach proposed recently by Kamary et al. [2014] where hypotheses are the components of a mixture model and the posterior distribution of the mixing proportion is the outcome of the test. More specifically, they propose to model the observations \mathcal{D} by an encompassing mixture

model

$$\mathcal{D} \sim \alpha P(\mathcal{D}|\theta_0, M_0) + (1 - \alpha)P(\mathcal{D}|\theta_1, M_1) \quad (10)$$

with $0 \leq \alpha \leq 1$ the mixing proportion also to be inferred. Kamary et al. [2014] argues the posterior distribution on α allows for a more thorough assessment of the strength of the support of one model against the other comparing to the single numerical value given by the Bayes factor. It removes the artificial prior probabilities on model indices $P(M_0)$ and $P(M_1)$ required by Bayes factor computations. Most notably, the approach allows the use of noninformative priors when the two competing hypotheses share the same set of parameters. This was prohibitive in the classical Bayesian two-sample testing approach like Bayes factor [DeGroot, 1973].

In this work, we will adapt the classical Bayes factor approach to evaluate the evidence in favour of the null hypothesis. The mixture modelling formulation of the problem will be left as future work. The two-sample testing problem in the most general form as presented above need not have $n_x = n_y$. For simplicity, we restrict our attention to the paired two-sample testing problem, i.e. $\{(x_i, y_i)\}_{i=1}^n$. Instead of considering the observations directly, we propose to work with the difference between the two distributions' mean embeddings in the RKHS. In the kernel literature, this quantity is proportional to the witness function of the two-sample test statistic Maximum Mean Discrepancy [Gretton et al., 2012a, Definition 2].

Inspired by the work of Flaxman et al. [2016] where the distribution mean embedding is modelled with a Gaussian process prior and a normal likelihood, we use a similar model for the difference between the kernel mean embeddings. Intuitively, to model the kernel mean embedding for X (or for Y) directly with a GP prior is not ideal as kernel mean embeddings for a non-negative kernel (like Gaussian kernel and Matérn kernel) are never negative, but the draws from any GP prior can be negative. Hence, it seems more suitable to place a prior directly on the difference between the mean embeddings as we do in this contribution. A further advantage of modelling the difference is that we will no longer require the independence assumption between the random variables X and Y . Such assumption is common in two-sample testing literature both in the frequentist and the Bayesian setting,

in particular, a two-sample test based on MMD requires such assumption.

2 Kernel Mean Embeddings

Before introducing the proposed model, we will first review the notion of a reproducing kernel Hilbert space (RKHS) and the corresponding reproducing kernel. This will enable us to introduce the key concept for our method – the kernel mean embedding. For more detailed treatment of the subject, we refer the readers to Berlinet and Thomas-Agnan [2004], Steinwart and Christmann [2008], Sriperumbudur [2010].

Definition 2.1. [Steinwart and Christmann, 2008, Definition 4.18] *Let \mathcal{Z} be any topological space on which Borel measures can be defined. Let \mathcal{H} be a Hilbert space of real-valued functions defined on \mathcal{Z} . A function $k : \mathcal{Z} \times \mathcal{Z} \rightarrow \mathbb{R}$ is called a **reproducing kernel** of \mathcal{H} if:*

1. $\forall z \in \mathcal{Z}, k(\cdot, z) \in \mathcal{H}$
2. $\forall z \in \mathcal{Z}, \forall f \in \mathcal{H}, \langle f, k(\cdot, z) \rangle_{\mathcal{H}} = f(z)$. (The Reproducing Property)

If \mathcal{H} has a reproducing kernel, it is called a **Reproducing Kernel Hilbert Space (RKHS)**.

The reproducing property allows the reproducing kernel to be written as

$$k(x, y) = \langle k(\cdot, x), k(\cdot, y) \rangle_{\mathcal{H}} \quad (11)$$

for all $x, y \in \mathcal{Z}$. Reproducing kernels can be defined on graphs, text, images, strings, probability distributions as well as Euclidean domains [Shawe-Taylor and Cristianini, 2004]. For Euclidean domain \mathbb{R}^d , the Gaussian RBF kernel $k(x, y) = \exp\left(-\frac{1}{2\sigma^2}\|x - y\|^2\right)$ with lengthscale $\sigma > 0$ is an example of a reproducing kernel.

Probability distributions can be represented as elements of a RKHS and they are known as the kernel mean embeddings [Berlinet and Thomas-Agnan, 2004, Smola et al., 2007]. This setting has been particularly useful in the kernel nonparametric two-sample testing framework [Borgwardt et al., 2006, Gretton et al., 2012a] since discrepancies between two

distributions can be written succinctly as the square Hilbert-Schmidt norm between their respective kernel mean embeddings. More formally, kernel mean embeddings can be defined as follows.

Definition 2.2. *Let k be a kernel on \mathcal{Z} , and $\nu \in \mathcal{M}_+^1(\mathcal{Z})$ with $\mathcal{M}_+^1(\mathcal{Z})$ denoting the set of Borel probability measures on \mathcal{Z} . The **kernel embedding** of probability measure ν into the RKHS \mathcal{H}_k is $\mu_k(\nu) \in \mathcal{H}_k$ such that*

$$\int f(z) d\nu(z) = \langle f, \mu_k(\nu) \rangle_{\mathcal{H}_k}, \quad \forall f \in \mathcal{H}_k. \quad (12)$$

In other words, the kernel mean embedding can be written as $\mu_k(\nu) = \int k(\cdot, z) d\nu(z)$, i.e. any probability measure is mapped to the corresponding expectation of the canonical feature map $k(\cdot, z)$ through the kernel mean embedding. When the kernel k is measurable on \mathcal{Z} and $\mathbb{E}(\sqrt{k(z, z)}) < \infty$, the existence of the kernel mean embedding is guaranteed [Gretton et al., 2012a, Lemma 3]. Further, Fukumizu et al. [2008] showed that when the corresponding kernels are characteristic, the mean embedding maps are injective and hence preserve all information of the probability measure. An example of a characteristic kernel is the Gaussian kernel on the entire domain of \mathbb{R}^d .

3 Proposed Method

Consider a paired data set $\mathcal{D} = \{(x_i, y_i)\}_{i=1}^n$ with $x_i, y_i \in \mathcal{X}$ for some generic domains \mathcal{X} . Further, let $x_i \stackrel{i.i.d.}{\sim} P$ and $y_i \stackrel{i.i.d.}{\sim} Q$ for some unknown distributions P and Q . Let $k_\theta(\cdot, \cdot)$ be a positive definite kernel parameterised by θ , with the corresponding reproducing kernel Hilbert space \mathcal{H} .

In this work, we develop a Bayesian two-sample test based on the difference between the kernel mean embeddings. We consider the empirical estimate of such difference evaluated at a set of locations and propose a Bayesian inference scheme so that the relative evidence in favour of H_0 and H_1 is quantified. The proposed test is conditional on the choice of the family of kernels parameterised by θ . We focus on working with the Gaussian RBF kernel in this contribution, but other kernels are readily applicable to the framework developed

here. To emphasize the dependence of the kernel function on the lengthscale parameter θ , we write $k_\theta(\cdot, \cdot)$. Denote the respective kernel mean embeddings for X and Y as

$$\mu_X = \mathbb{E}_X(k_\theta(\cdot, X)) = \int_{\mathcal{X}} k_\theta(\cdot, x) P(dx), \quad (13)$$

$$\mu_Y = \mathbb{E}_Y(k_\theta(\cdot, Y)) = \int_{\mathcal{Y}} k_\theta(\cdot, y) Q(dy), \quad (14)$$

with the empirical estimators and the corresponding estimates denoted by

$$\hat{\mu}_X = \frac{1}{n} \sum_{i=1}^n k_\theta(\cdot, X_i) \quad \text{and} \quad \hat{\mu}_x = \frac{1}{n} \sum_{i=1}^n k_\theta(\cdot, x_i), \quad (15)$$

$$\hat{\mu}_Y = \frac{1}{n} \sum_{i=1}^n k_\theta(\cdot, Y_i) \quad \text{and} \quad \hat{\mu}_y = \frac{1}{n} \sum_{i=1}^n k_\theta(\cdot, y_i). \quad (16)$$

We denote the witness function up to proportionality as $\delta = \mu_X - \mu_Y$, which is simply the difference between the kernel mean embeddings. Under the null hypothesis, the two distributions P and Q are the same and with the use of characteristic kernels, all information of the probability distribution is preserved through the kernel mean embeddings μ_X and μ_Y . Hence, the null hypothesis is equivalent to $\delta = 0$ and the alternative is equivalent to $\delta \neq 0$.

Given the set of evaluation points $\mathbf{z} = \{z_i\}_{i=1}^p \in \mathcal{X}$, we define the evaluation of δ at \mathbf{z} as

$$\delta(z_i) = \mu_X(z_i) - \mu_Y(z_i) \quad (17)$$

$$= \mathbb{E}_X(k_\theta(z_i, X)) - \mathbb{E}_Y(k_\theta(z_i, Y)), \quad \forall i = 1, \dots, p \quad (18)$$

$$\delta(\mathbf{z}) = (\delta(z_1), \dots, \delta(z_p))^\top \in \mathbb{R}^p. \quad (19)$$

Such evaluations $\delta(\mathbf{z})$ will act as the quantity of interest of our proposed model, while the empirical estimate of $\delta(\mathbf{z})$ on a given set of data $\mathcal{D} = \{(x_i, y_i)\}_{i=1}^n$ will be regarded as the observations. This will be made precise in the following sections. Ideally, half of the evaluation points $\mathbf{z} = \{z_i\}_{i=1}^p$ are sampled from P , while the other half are sampled from Q . When direct sampling is not possible (e.g. when we have access to the distributions only through samples), the evaluation points are subsampled from the given data set. We

define the p -dimensional witness vector Δ as the empirical estimate of $\delta(\mathbf{z})$:

$$\Delta = \{\hat{\mu}_x(z_j) - \hat{\mu}_y(z_j)\}_{j=1}^p \quad (20)$$

$$= \left\{ \frac{1}{n} \sum_{i=1}^n k_\theta(x_i, z_j) - \frac{1}{n} \sum_{i=1}^n k_\theta(y_i, z_j) \right\}_{j=1}^p \quad (21)$$

$$= \left\{ \frac{1}{n} \sum_{i=1}^n (k_\theta(x_i, z_j) - k_\theta(y_i, z_j)) \right\}_{j=1}^p. \quad (22)$$

and the corresponding random variable as $\Delta_{XY} := \{\hat{\mu}_X(z_j) - \hat{\mu}_Y(z_j)\}_{j=1}^p$.

Following the classical Bayesian two-sample testing framework, we will quantify the evidence in favour of the two-sample coming from the same distribution vs different distributions through Bayes factor. However, in contrast to (4) and (5), the independence assumption between random variables X and Y is no longer assumed and hence we compute the Bayes factor as

$$BF = \frac{P(\Delta|H_0)}{P(\Delta|H_1)} = \frac{P(H_0|\Delta)P(H_1)}{P(H_1|\Delta)P(H_0)}. \quad (23)$$

We introduce the parameter $M = \{0, 1\}$, such that $M = 0$ indicates the null hypothesis and $M = 1$ indicates the alternative hypothesis. (23) can be written as

$$BF = \frac{P(\Delta|M=0)}{P(\Delta|M=1)} = \frac{P(M=0|\Delta)P(M=1)}{P(M=1|\Delta)P(M=0)}. \quad (24)$$

Following the Bayesian kernel embeddings approach of Flaxman et al. [2016], we propose to model δ with a Gaussian process (GP) prior under the alternative model in Section 4. Assuming a Gaussian noise model, we derive the marginal likelihood of Δ for fixed kernel lengthscale parameter θ . When such a parameter is unknown, the framework of Flaxman et al. [2016] enables the derivation of the posterior distribution of the parameter given the observations. To alleviate the heavy computation burden of computing the marginal likelihood of the dataset $\{(x_i, y_i)\}_{i=1}^n | \theta$, we propose an alternative formulation of the likelihood utilising the Kronecker product structure of our problem in the Supplementary Material. Under the null hypothesis (Section 5), the model simplifies significantly due to the zeroing of δ , i.e. we pose a Gaussian noise model for $\Delta | \theta$ directly. The fast computation of the marginal likelihood mimics the derivation in the case of the alternative model which is

also presented in the Supplementary Material. Common to both the null and alternative model are the estimation of the covariance matrix of the noise model and the computation of the Jacobian matrix. In the Supplementary Material, we details two estimation methods of the covariance matrix of the noise model different from the isotropic model used in Flaxman et al. [2016]. In addition, we derive the formulas for the Jacobian computation. Section 6 proposes a Metropolis Hasting within Gibbs type of approach for inferring the posterior distribution of θ and that of the model given the observed data. Section 7 studies the performance of the proposed method on various synthetic data experiments. Section 8 presents the results on two real data experiments where we test network heterogeneity from high dimensional data in the first experiment and compare six-membered monocyclic ring conformation under two different conditions in the second experiment.

4 Alternative Model

Under the alternative hypothesis, $\delta = \mu_X - \mu_Y \neq 0$. We propose to model the unknown quantity δ using a Gaussian Process (GP) prior. Draws from a naively defined prior $\mathcal{GP}(0, k_\theta(\cdot, \cdot))$ would almost surely fall outside of the RKHS \mathcal{H} that corresponds to $k_\theta(\cdot, \cdot)$ [Wahba, 1990]. Hence, Flaxman et al. [2016] proposed to define the GP prior as

$$\delta | \theta \sim \mathcal{GP}(0, r_\theta(\cdot, \cdot)) \quad (25)$$

with the covariance operator $r_\theta(\cdot, \cdot)$ defined as

$$r_\theta(z, z') := \int k_\theta(z, u) k_\theta(u, z') \nu(du) \quad (26)$$

where ν is any finite measure on \mathcal{X} . Using results from Lukić and Beder [2001] and Theorem 4.27 of Steinwart and Christmann [2008], Flaxman et al. [2016] show that such choice of r_θ ensures that $\delta \in \mathcal{H}$ with probability 1 by the nuclear dominance for k_θ over r_θ for any stationary kernel k_θ and more generally $\int k_\theta(x, x) \nu(dx) < \infty$. Intuitively, the new covariance operator r_θ is a smoother version of k_θ since it is the convolution of k_θ with itself with respect to a finite measure ν [Flaxman et al., 2016]. For our particular choice of k_θ being a Gaussian RBF kernel on $\mathcal{X} = \mathbb{R}^D$, Flaxman et al. [2016] showed (in A.3) that

the covariance function r_θ of square exponential kernels

$$k_\theta(x, y) = \exp\left(-\frac{1}{2}(x - y)^\top \tilde{\Sigma}_\theta^{-1}(x - y)\right) \quad (27)$$

with $x, y \in \mathbb{R}^D$ and diagonal covariance $\tilde{\Sigma}_\theta = \theta I = (\theta^{(1)}, \dots, \theta^{(D)})^\top I$ can be written as

$$r_\theta(x, y) = \pi^{D/2} \left(\prod_{d=1}^D \theta^{(d)} \right)^{1/2} \exp\left(-\frac{1}{2}(x - y)^\top (2\theta I_D)^{-1}(x - y)\right). \quad (28)$$

When $\theta^{(1)} = \dots = \theta^{(D)} = \theta$, the above can be further simplified as

$$r_\theta(x, y) = \pi^{D/2} \theta^{D/2} \exp\left(-\frac{1}{4\theta}(x - y)^\top (x - y)\right). \quad (29)$$

We will use this form of the covariance function in our experiments.

Given the set of evaluation points $\{z_j\}_{j=1}^p$, the prior translates into a p -dimensional multivariate Gaussian distribution

$$\delta(\mathbf{z})|\theta \sim N(0, R_\theta) \quad (30)$$

with $[R_\theta]_{ij} = r_\theta(z_i, z_j)$. We link the empirical estimate Δ with the true differences δ evaluated at this set of evaluation points through a Gaussian likelihood of the model. This is an approximation of the true likelihood which hinges on the common “Gaussianity in the feature space” assumption in the kernel method literature and is also utilised in Flaxman et al. [2016]. We write it as

$$\Delta_{XY}|\delta, \theta \sim \mathcal{N}([\delta(z_1), \dots, \delta(z_p)]^\top, \frac{1}{n}\Sigma_\theta). \quad (31)$$

We details two ways to estimated Σ_θ empirically in the Supplementary Material. The constant $\frac{1}{n}$ is for notational convenience to be seen later. Integrating out the prior distribution of δ , we obtain the marginal likelihood

$$\Delta_{XY}|\theta \sim \mathcal{N}(0_p, R_\theta + \frac{1}{n}\Sigma_\theta). \quad (32)$$

For the purpose of hyperparameter learning, we would like to compute the posterior distribution of $\theta|\{(x_i, y_i)\}_{i=1}^n$. As a first step, we will need to integrate out the model parameter δ and compute the marginal probability of the observations $\{(x_i, y_i)\}_{i=1}^n$ given

the hyperparameter θ . Note that Δ_{XY} implicitly depends on the parameter θ through the kernel functions, hence we follow the exposition of Flaxman et al. [2016] to apply a change of variables such that the θ dependence is separated out.

For every fixed pair of (x_i, y_i) , define the finite dimensional feature map $\phi_\theta : \mathbb{R}^D \rightarrow \mathbb{R}^p$ as

$$\phi_\theta(x) - \phi_\theta(y) = [k_\theta(x, z_1) - k_\theta(y, z_1), \dots, k_\theta(x, z_p) - k_\theta(y, z_p)]^\top \in \mathbb{R}^p. \quad (33)$$

Note, $k_\theta(X_i, z_j) - k_\theta(Y_i, z_j)$ are independent for all $i = 1, \dots, n$ given δ . This implies that $n\Delta_{XY}$ can be written as a sum of independent random variables: $\Delta_{XY} = \frac{1}{n} \sum_{i=1}^n (\phi_\theta(X_i) - \phi_\theta(Y_i))$. By Cramer's decomposition theorem, we obtain the distribution of each of the contributing components

$$\phi_\theta(X_i) - \phi_\theta(Y_i) | \delta, \theta \sim \mathcal{N}([\delta_\theta(z_1), \dots, \delta_\theta(z_p)]^\top, \Sigma_\theta). \quad (34)$$

Applying the change of variable $(x, y) \mapsto g_\theta(x, y) := (\phi_\theta(x) - \phi_\theta(y))$ and using the generalisation of the change-of-variable formula to non-square Jacobian matrices [Ben-Israel, 1999] to obtain a distribution for (x, y) conditionally on δ

$$p(x, y | \delta, \theta) = p(g_\theta(x, y) | \delta, \theta) \text{vol}[J_\theta(x, y)]. \quad (35)$$

The Jacobian J_θ is a $p \times 2D$ matrix with

$$J_\theta(x, y) = \begin{cases} \frac{\partial g_\theta(x, y)_{z_i}}{\partial x^j}, & \text{for } j = 1, \dots, D \\ \frac{\partial g_\theta(x, y)_{z_i}}{\partial y^j}, & \text{for } j = D + 1, \dots, 2D \end{cases} \quad (36)$$

and $\text{vol}[J_\theta(x, y)] := \sqrt{\det(J_\theta(x, y)^\top J_\theta(x, y))}$. This can be further simplified into

$$J_\theta(x, y) = \begin{cases} \frac{\partial k_\theta(x, z_i)}{\partial x^j}, & \text{for } j = 1, \dots, D \\ \frac{\partial k_\theta(y, z_i)}{\partial y^j}, & \text{for } j = D + 1, \dots, 2D. \end{cases} \quad (37)$$

The detailed computation of the Jacobian matrix will be discussed in Supplementary Material. By the conditional independence of $g(x_i, y_i)$ for each i given δ and noting that θ

represents the hyperparameter of the kernel $k_\theta(\cdot, \cdot)$, then

$$\begin{aligned}
p(\{x_i, y_i\}_{i=1}^n | \delta, \theta) &= \prod_{i=1}^n p(g_\theta(x_i, y_i) | \delta, \theta) \text{vol}[J_\theta(x_i, y_i)] \\
&= \prod_{i=1}^n \mathcal{N}(g_\theta(x_i, y_i); \delta_\theta(\mathbf{z}), \Sigma_\theta) \text{vol}[J_\theta(x_i, y_i)] \\
&= \mathcal{N}(\text{vec}(G_\theta); m_\theta(\mathbf{z}), I_n \otimes \Sigma_\theta) \prod_{i=1}^n \text{vol}[J_\theta(x_i, y_i)]
\end{aligned} \tag{38}$$

where $G_\theta = [g_\theta(x_1, y_1), \dots, g_\theta(x_n, y_n)]$ is a $p \times n$ matrix and $\text{vec}(G_\theta) \in \mathbb{R}^{np}$ is the vectorisation of the matrix G_θ . The mean vector $m_\theta(\mathbf{z}) := [\delta_\theta(\mathbf{z})^\top \dots \delta_\theta(\mathbf{z})^\top]^\top$ where each $\delta_\theta(\mathbf{z}) = [\delta(z_1), \dots, \delta(z_p)]^\top$. To obtain the marginal pseudolikelihood of $p(\{(x_i, y_i)\}_{i=1}^n | \theta)$, we compute the integral

$$\begin{aligned}
p(\{(x_i, y_i)\}_{i=1}^n | \theta) &= \int p(\{(x_i, y_i)\}_{i=1}^n | \delta, \theta) p(\delta | \theta) d\delta \\
&= \int \mathcal{N}(\text{vec}(G_\theta); m_\theta(\mathbf{z}), I_n \otimes \Sigma_\theta) \mathcal{N}(\delta; 0, R_\theta) \prod_{i=1}^n \text{vol}[J_\theta(x_i, y_i)] d\delta \\
&= \mathcal{N}(\text{vec}(G_\theta); 0, \mathbb{1} \mathbb{1}^\top \otimes R_\theta + I_n \otimes \Sigma_\theta) \prod_{i=1}^n \text{vol}[J_\theta(x_i, y_i)].
\end{aligned} \tag{39}$$

The term ‘‘pseudolikelihood’’ is used since it relies on the evaluation of the empirical embedding at a finite set of inducing points and hence it is an approximation to the likelihood of the infinite dimensional empirical embedding [Flaxman et al., 2016].

Although the derivations presented here follow essentially the same steps as Flaxman et al. [2016], it is important to note that different from Flaxman et al. [2016], we model the difference between the empirical mean embeddings of the two distributions of interest rather than the embedding of a single distribution. This has several implications. As discussed in Flaxman et al. [2016], the marginal pseudolikelihood involves the computation of the inverse and the log determinant of an np -dimensional matrix. A naive direct implementation would require a prohibitive computation of $\mathcal{O}(n^3 p^3)$. Since we consider the difference between the empirical mean embeddings, the efficient computation utilising eigendecompositions of the relevant matrices [Flaxman et al., 2016, A.4] cannot be applied directly. Fortunately, the special form of the corresponding $np \times np$ covariance matrix allows faster computation

following Kronecker product algebra and the applications of matrix determinant lemma and Woodbury identity. We pose detail the derivation in the Supplementary Material.

Utilising the proposed efficient computation, the log marginal pseudolikelihood (4) can be written as

$$\begin{aligned}
& \log p(\{(x_i, y_i)\}_{i=1}^n | \theta) \\
&= \text{const} + -\frac{1}{2} \log \det(\Sigma_\theta + nR_\theta) - \frac{1}{2}(n-1) \log \det(\Sigma_\theta) \\
&\quad - \frac{1}{2} \text{Tr} \left((\Sigma_\theta + nR_\theta)^{-1} G_\theta G_\theta^\top + \left(\frac{1}{n} \Sigma_\theta R_\theta^{-1} \Sigma_\theta + \Sigma_\theta \right)^{-1} G_\theta H G_\theta^\top \right) \\
&\quad + \frac{1}{2} \sum_{i=1}^n \log \det(J_\theta(x_i, y_i)^\top J_\theta(x_i, y_i)). \tag{40}
\end{aligned}$$

5 Null Model

In this section, we derive the marginal pseudolikelihood under the null model. The model simplifies significantly as $\delta = 0$, we propose to model the data directly with a Gaussian noise model

$$\Delta | \theta \sim \mathcal{N}(0, \frac{1}{n} \Sigma_\theta) \tag{41}$$

where as before, we rewrite the covariance matrix as $\frac{1}{n} \Sigma_\theta$. By a similar argument as in Section 4, we obtain

$$g_\theta(x_i, y_i) | \theta \sim \mathcal{N}(0, \Sigma_\theta) \tag{42}$$

for $i = 1, \dots, n$. This implies that the marginal pseudolikelihood can be written as

$$p(\{x_i, y_i\}_{i=1}^n | \theta) = \prod_{i=1}^n p(g_\theta(x_i, y_i) | \theta) \text{vol}(J_\theta(x_i, y_i)) \tag{43}$$

$$= \mathcal{N}(\text{vec}(G_\theta); 0, I_n \otimes \Sigma_\theta) \prod_{i=1}^n \text{vol}(J_\theta(x_i, y_i)). \tag{44}$$

A naive computation of the above again incur a prohibitive computational burden that scales like $\mathcal{O}(p^3 n^3)$. We mimic the case of the alternative model and derive the efficient

computation of the exponential term of marginal pseudolikelihood (as presented in the Supplementary Material). For the log determinant term, $\det(I_n \otimes \Sigma_\theta) = \det(I_n)^m \otimes \det(\Sigma_\theta)^n$ by properties of matrix determinant. Since the $\det(I_n)^m = 1$, then the marginal pseudolikelihood can be written as

$$\begin{aligned} \log p(\{x_i, y_i\}_{i=1}^n | \theta) \\ \propto -0.5n \log(\det(\Sigma_\theta)) - 0.5\text{Tr}(\Sigma_\theta^{-1}GG^\top) + \sum_{i=1}^n \log \text{vol}(J_\theta(x_i, y_i)). \end{aligned} \quad (45)$$

6 Posterior Inference

When the lengthscale parameter θ is fixed, the computation of the posterior distribution of $M|\mathcal{D}$ is straightforward. However, a wrong choice of such lengthscale parameter can hurt the performance of the proposed Bayesian test (examples of which are presented in the Supplementary Material). In this section, we propose to use a Metropolis Hasting within Gibbs type of approach for the joint posterior inference of M and θ . Iteratively, we would like to sample from $p(\theta|M, \mathcal{D})$ and $p(M|\theta, \mathcal{D})$.

To sample from $p(\theta|M, \mathcal{D})$, we can evaluate $\log p(\theta|\{(x_i, y_i)\}_{i=1}^n, M)$ by adding the log prior distribution $\text{Gamma}(2, 2)$ to the log marginal pseudolikelihood of the alternative model (40) and that of the null model (45). To sample from $p(M|\theta, \mathcal{D})$, recall the relationship between Bayes factor and the posterior distribution of the null (6) and alternative model (7) respectively

$$\begin{aligned} p(M = 1|\theta, \mathcal{D}) &= \frac{1}{1 + BF_\theta}, \\ p(M = 0|\theta, \mathcal{D}) &= \frac{BF_\theta}{1 + BF_\theta}. \end{aligned}$$

We index BF of (24) by θ to emphasize the dependence of the Bayes factor on the kernel hyperparameter θ , i.e.

$$BF_\theta = \frac{P(\Delta|M = 0, \theta)}{P(\Delta|M = 1, \theta)}. \quad (46)$$

Equivalently, this says $M|\theta, \mathcal{D} \sim \text{Bernoulli}\left(\frac{1}{1+BF_\theta}\right)$.

We present pseudocode of our posterior inference procedure in Algorithm 1. We observe from our experiments, that increasing the number of HMC steps inside Gibbs \tilde{n} improves the posterior convergence of the chain. The posterior marginal probability $P(\theta|\mathcal{D})$ is approximated by the posterior MCMC samples $\{\theta_1, \dots, \theta_{\tilde{m}}\}$. On the other hand, the posterior marginal probability $P(M = 1|\mathcal{D})$ is the proportion of $M = 1$ in all the samples $\{M_0, \dots, M_{\tilde{m}}\}$.

Data: A paired sample $\mathcal{D} = \{x_i, y_i\}_{i=1}^n$; The number of inducing points m ; The number of simulation \tilde{m} ; The number of HMC steps \tilde{n} .

Output: A sample $\{\theta_i, M_i\}_{i=1}^{\tilde{m}}$ from the posterior distribution of $p(\theta, M|\mathcal{D})$.

```

1 Initialise  $\theta_0$  = Median heuristic on the set  $\{x_1, \dots, x_n, y_1, \dots, y_n\}$ ;
2 Initialise  $M_0$  by computing the Bayes factor (BF) in (46) and sample
    $Bernoulli(\frac{1}{1+BF_\theta})$ ;
3 for  $i \leftarrow 1$  to  $\tilde{m}$  do
4   Simulate a chain  $\{\theta_1, \dots, \theta_{\tilde{n}}\}$  from  $p(\theta|M_{i-1}, \mathcal{D})$  using NUTS in Stan;
5   Set  $\theta_i = \theta_{\tilde{n}}$ ;
6   Simulate  $M_i \sim Bernoulli\left(\frac{1}{1+BF_\theta}\right)$  ;
7 end

```

Algorithm 1: Posterior Inference of the lengthscale parameter θ of the Gaussian RBF kernel and the model indicator M .

7 Synthetic Data Experiments

In this section, we would like to investigate the performance of the proposed posterior inference scheme for M and θ on synthetic data experiments. For each of the synthetic experiments, we generate 100 independent data sets of size n for each of the models. We examine the distribution of the probability of the alternative hypothesis (i.e. $p(M = 1|\mathcal{D})$) while varying the number of observed data points n . The number of evaluation points is fixed at $p = 40$, with half sampled from the distribution of X and the other half sampled from the distribution of Y .

For the posterior sampling, we run the algorithm for $\tilde{m} = 2000$. The initial 500 samples

are discarded as burn-in and the thinning factor is 2. For every Gibbs sampling step, we take 9 steps in HMC which contains 3 warmup steps for step size adaption. Note, we have experimented with 1 HMC step for every step of Gibbs sampling, the convergence of the parameters M and θ is much slower in that case. On the other hand, increasing the number of HMC steps beyond 9 does not seem to improve the performance by a significant amount. We used 9 steps for a balance between computational complexity and performance.

7.1 Simple 1 Dimensional Distributions

7.1.1 Gaussian Distributions

This section investigates if the proposed method is able to detect the change in mean and/or variance of simple 1-dimensional Gaussian distributions. We present the results of two cases in Figure 1 when $X \stackrel{i.i.d.}{\sim} \mathcal{N}(0, 1)$ and $Y \stackrel{i.i.d.}{\sim} \mathcal{N}(0, 9)$ or $Y \stackrel{i.i.d.}{\sim} \mathcal{N}(1, 1)$. The null case and some other alternative cases are presented in the Supplementary Material for the interested reader. When there is a difference in the variance of the Gaussian distribution, for example when the alternative model is $\mathcal{N}(0, 9)$, the probability of $M = 1$ is zero when 50 or 100 samples are given. As we increase the sample size to 200, we observe that the test is almost certain since probability of $M = 1$ varying from 0.65 to approximately 1 with median at around 0.85. However, as we increase the sample size to 500, the probability of $M = 1$ is more concentrated towards 1. This phenomena is observed for all the alternative models considered.

Essentially, when the number of samples is small, there is not enough evidence to determine if the null hypothesis should be rejected. In such a case, the Bayes factor favours the simpler null hypothesis. This is to be expected since Bayesian modelling encompasses a natural Occam factor in the prior predictive [MacKay, 2003, Chapter 28]. We will see this reflected in all the synthetic experiments in this section. Note, for a Gaussian distribution, the difference in mean is easier to detect comparing to a difference in variance. This is reflected in the results presented here and in the Supplementary Material: we observe that the probability of the alternative hypothesis becomes very close to 1 at a much smaller sample size for the experiments with a difference in mean.

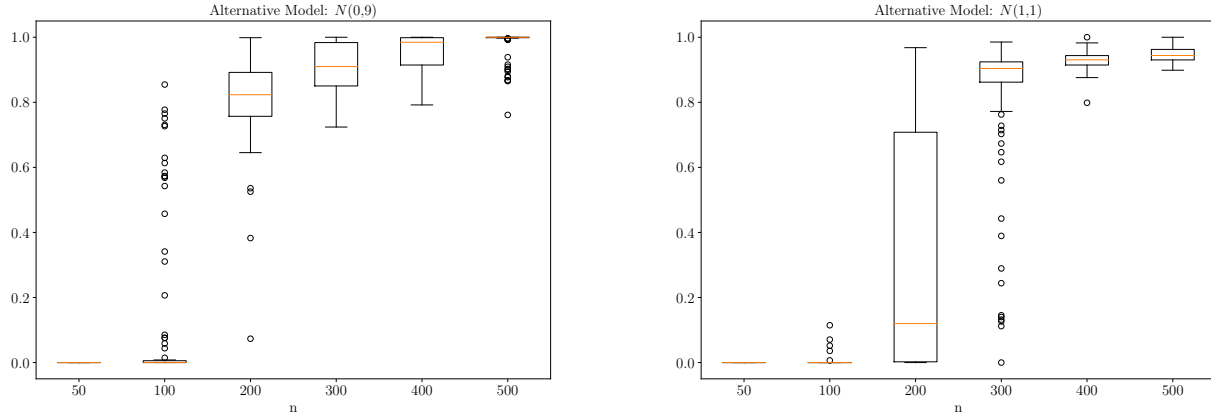


Figure 1: 1-dimensional Gaussian experiment: distribution (over 100 independent runs) of the probability of the alternative hypothesis $p(M = 1|\mathcal{D})$ for a different number of observations n . The null hypothesis is both samples X and Y are i.i.d. $\mathcal{N}(0, 1)$ and the alternative hypothesis is $Y \stackrel{i.i.d.}{\sim} \mathcal{N}(0, 9)$ (Left) and $Y \stackrel{i.i.d.}{\sim} \mathcal{N}(1, 1)$ (Right). As expected, the proposed method is able to detect the difference between the given samples.

We emphasize that, unlike the frequentist kernel two-sample test where a single value of the lengthscale parameter needs to be predetermined, the proposed Bayesian framework integrates over all possible θ values and alleviates the need for kernel lengthscale selection. However, some θ values are more informative in distinguishing the difference between the two distributions while others are less informative. As a specific example, we consider the case when $X \sim \mathcal{N}(0, 1)$ and $Y \sim \mathcal{N}(0, 9)$ with 200 samples each. For this specific simulation, we obtain $P(M = 1|\mathcal{D}) \approx 0.839$. Figure 2 illustrates the change of the probability of $M = 1|\theta, \mathcal{D}$ as a function of θ . Clearly, the region of θ from approximately 0.05 to 11 is most informative for distinguishing these two distributions. This is also reflected in the marginal distribution of $\theta|M = 1$ and $\theta|M = 0$ from Figure 3. Rather than selecting a single lengthscale parameter, the proposed method is able to highlight the range of informative lengthscales. As we will see, this is more useful in cases when multiple lengthscale parameters are of interest for a single testing problem.

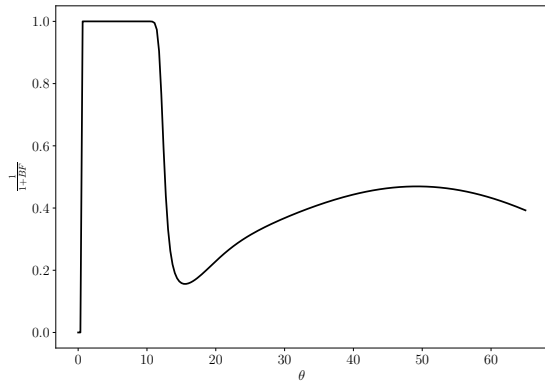


Figure 2: 1-dimensional Gaussian experiment with the alternative model $Y \stackrel{i.i.d.}{\sim} \mathcal{N}(0, 9)$ and 200 samples. The plot illustrates $\frac{1}{1+BF_\theta}$ as a function of θ .

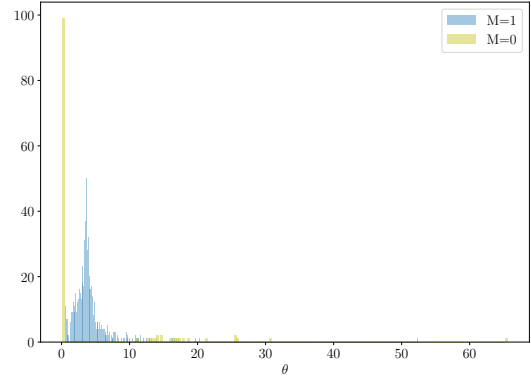


Figure 3: 1-dimensional Gaussian experiment with the alternative model $Y \stackrel{i.i.d.}{\sim} \mathcal{N}(0, 9)$ and 200 samples. The histogram of $\theta | M, \mathcal{D}$ for $M = 1$ and $M = 0$.

7.1.2 Laplace Distributions

We consider comparing the standard Normal distribution $\mathcal{N}(0, 1)$ against $Laplace(0, 1.5)$ and $Laplace(0, 0.4)$. The results are presented in Figure 4 which aligns with our expectation. As the number of samples increases the test is becoming increasing certain of the difference between our null and alternative model and hence concentrate $P(M = 1 | \mathcal{D})$ at 1. Since the proposed method is not restricted to two-sample testing between independent random variables, we also consider the same experiment with correlated standard Gaussian and Laplace distributions generated through copula transformation with correlation set to 0.5. The correlated structure has helped the discovery of the difference between the distributions. Results are presented in Supplementary Material illustrating that the method works equally well in correlated random variable cases.

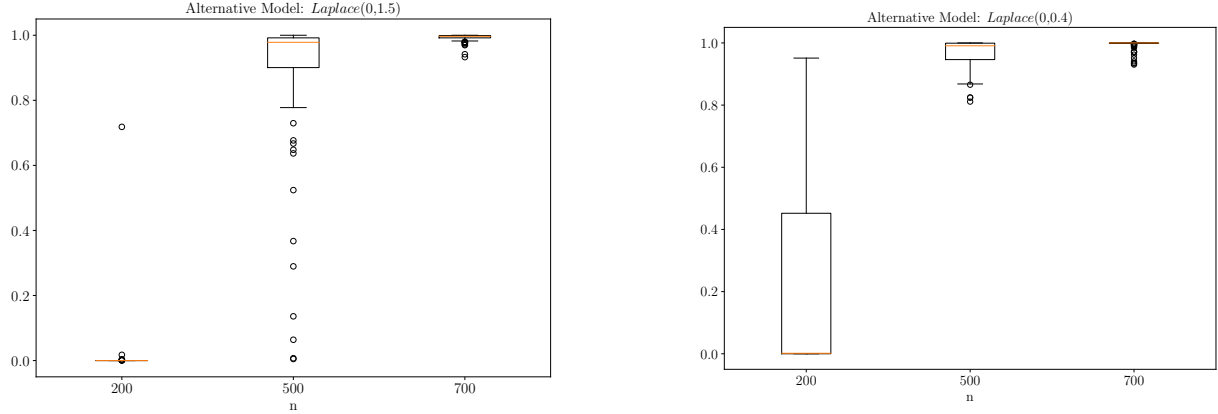


Figure 4: 1-dimensional Laplace experiment: distribution (over 100 independent runs) of the probability of the alternative hypothesis $p(M = 1 | \mathcal{D})$ for a different number of observations n . The null hypothesis is both samples X and Y are i.i.d. $\mathcal{N}(0, 1)$ and the alternative hypothesis is $Y \stackrel{i.i.d.}{\sim} \text{Laplace}(0, 1.5)$ (Left) and $Y \stackrel{i.i.d.}{\sim} \text{Laplace}(0, 0.4)$ (Right).

7.2 2 Dimensional Gaussian Distributions

Before investigating examples where multiple lengthscales are of interest, we first consider the Gaussian distributions in 2 dimensions with

$$X \sim \mathcal{N} \left(\begin{pmatrix} 10 \\ 10 \end{pmatrix}, \begin{pmatrix} 1 & 0 \\ 0 & 1 \end{pmatrix} \right) \quad (47)$$

$$Y \sim \mathcal{N} (M_y, Q S_\epsilon Q^\top) \quad (48)$$

where $M_y \in \mathbb{R}^2$ is the mean vector, Q is the rotation matrix

$$Q = \begin{pmatrix} \cos(\frac{\pi}{2}) & \sin(\frac{\pi}{2}) \\ -\sin(\frac{\pi}{2}) & \cos(\frac{\pi}{2}) \end{pmatrix} \quad (49)$$

and S_ϵ is the diagonal matrix of the form

$$S_\epsilon = \begin{pmatrix} \epsilon & 0 \\ 0 & 1 \end{pmatrix}. \quad (50)$$

For the ease of notation, we denote $\Sigma(\epsilon) := Q S_\epsilon Q^\top$ highlighting the dependency on the parameter ϵ . More specifically, we consider the following parameter settings for the simulated data as shown in Table 1. Only the results from the first and the fourth cases of the

Y distributions are presented in the main text while the others are in the Supplementary Materials. Under the null hypothesis, we simulated both X and Y independently from a

	Null	Alternative					
M_y^\top	(10, 10)	(11.5, 11.5)	(12, 10)	(10, 10)	(10, 10)	(10, 10)	(10, 10)
ϵ	1	1	1	2	6	10	20

Table 1: The different parameters for the 2-dimensional Gaussian distribution experiment.

2 dimensional Gaussian distribution with $M_y = (10, 10)^\top$ and $\epsilon = 1$. As expected, the distribution of the probability of $M = 1$ is consistently zero for all sample sizes. Under the alternative hypothesis, as expected, we observe in Figure 5 that the probability distribution of the alternative hypothesis become concentrated around 1 as the number of samples increase. In other words, as more samples are seen, the Bayes factor is able to favor the alternative hypothesis with more certainty.

Note, for the case when $\epsilon = 2$, the difference between the two distributions is not detected even at the maximum sample size $n = 800$ considered and the Bayes factor consistently favours the null hypothesis. Since more samples are needed for the model to be able to detect the difference between the two distributions, we argue that large scale approximations such as random Fourier feature extension of the proposed method is needed. We will provide a brief discussion of this in Section 9.

7.3 Two by Two Blobs of 2-Dimensional Gaussian Distributions

The performance of the frequentist kernel two-sample test using MMD depends heavily on the choice of kernel. When a Gaussian kernel is used, this boils down to choosing an appropriate lengthscale parameter. Often, median heuristic is used. However, Gretton et al. [2012b] showed that MMD with median heuristic failed to reject the null hypothesis when comparing samples from a grid of isotropic Gaussian v.s. a grid of non-isotropic Gaussian. The framework proposed by Flaxman et al. [2016] showed, by choosing the lengthscale that optimise the Bayesian kernel learning marginal log likelihood (i.e. an empirical Bayes type of approach), MMD is able to correctly reject the null hypothesis at the desired significance

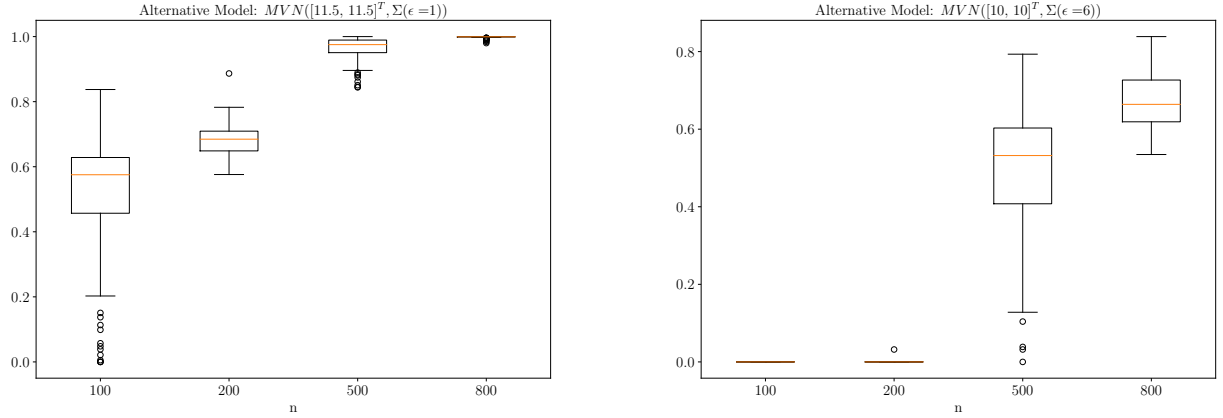


Figure 5: 2-dimensional Gaussian experiment: distribution (over 100 independent runs) of the probability of the alternative hypothesis $p(M = 1|\mathcal{D})$ for a different number of observations n . The null and alternative hypotheses are as shown in Table 1. We illustrate the results from the first (Left) and forth (Right) alternative model in the Table while the other ones are presented in the Supplementary Material.

level. Intuitively, the algorithm needs to look locally at each blob to detect the difference rather than at the lengthscale that covers all of the blobs which is given by the median distance between points.

We repeat this experiment using the proposed Bayesian two-sample test with P_X being a mixture of 2 dimensional isotropic Gaussian distributions and P_Y a mixture of 2 dimensional Gaussian distributions centered at slightly shifted locations with rotated covariance matrix. Note, this is not the same dataset used in Flaxman et al. [2016] and Gretton et al. [2012b], we shift the dataset to have multiple lengthscales relevant. We center the blobs of 2 dimensional Gaussian distributions of P_X at $\{(10, 10)^T, (10, 30)^T, (30, 10)^T, (30, 30)^T\}$ and shift such locations by $(-1, -1)$ for P_Y . An equal number of observations is sampled from each of the blobs. The covariance matrix of P_Y follows the same form as in Section 7.2 with $\epsilon = \{2, 6, 10, 20\}$. We present illustrations of the samples from these distributions in the Supplementary Material.

As an example, in Figure 7, we see that a wide range of lengthscales is informative for this two-sample testing problem when $\epsilon = 2$. If we further observe the marginal distri-

butions $P(\theta|M = 0, \mathcal{D})$ and $P(\theta|M = 1, \mathcal{D})$ in Figure 8, the method takes advantage of the large lengthscales to detect shift in location and the small lengthscales to detect the difference in covariance. But when the lengthscale is too small (approximately less than 0.5), the method regards the samples as identically distributed. Figure 6 shows that our approach is able to detect the difference between the distributions since the probability of the alternative hypothesis becomes more concentrated around 1 as the number of samples increases. Note, when $\epsilon = 2$, the distribution of the probability of the alternative hypothesis is around 0.6. We expect this to increase to 1 as we increase the number of samples to around 300 samples per blob given the pattern observed.

7.4 Higher Dimensional Gaussian Distributions

We have seen that the proposed method is able to utilise informative value of the lengthscale parameter and make correct decisions about the probability of the alternative hypothesis given large enough samples. In this section, we investigate the effect of dimensionality of the given sample on the proposed two-sample testing method. We use the Gaussian blobs experiment from the previous section and append simple $\mathcal{N}(0, 1)$ to both X and Y (i.e. the difference in distribution exists only in the first two dimensions). In particular, we consider the cases when the total number of dimensions are $\{3, 4, 5, 6, 7\}$. The results are presented in Figure 9.

Comparing to the plot of $\epsilon = 6$ from Figure 6 where no noise is added, the performance at 25 samples per blobs is very similar. At 75 samples per blobs, the posterior distribution is concentrated at 0 insisting the probability of the alternative hypothesis is zero. This is more conservative comparing to the $\epsilon = 6$ case of Figure 6 where the median of the distribution is around 0.4. At 125 samples per blob, the variance of the distribution of $\frac{1}{1+BF_\theta}$ increases and the median of the distribution of $\frac{1}{1+BF_\theta}$ decreases as the number of dimension increases from 2 to 7. Similarly, the first and third quantiles of the distribution also shift downward. At 200 samples per blob, we observe a similar performance as Figure 6. However, the medians of the distribution are slightly lower in higher dimensions. The noise in the additional dimensions has indeed made the problem harder for the given number of samples. But

the proposed method still manages to discover the difference as the number of samples increases. This illustrates the robustness of our proposed method to the dimensionality of the problem.

8 Real Data Experiments

8.1 Network Heterogeneity From High-Dimensional Data

In system biology and medicine, the dynamics of the data under analysis can often be described as a network of observed and unobserved variables, for example a protein signalling network in a cell [Städler and Mukherjee, 2019]. One interesting problem in this area is to investigate if the signalling pathways (networks) reconstructed from two subtypes are statistically different.

In this section, we follow the statistical setup given in Städler and Mukherjee [2017, 2019] and describes the networks by Gaussian graphical models (GGMs) which use an undirected graph (or network) to describe probabilistic relationships between p molecular variables. Assume that each sample X_i (and similarly for Y_i) is sampled from a multivariate Gaussian distribution with zero mean and some concentration matrix Ω (i.e. the inverse of a covariance matrix). The concentration matrix defines the graph G via

$$(j, j') \in E(G) \Leftrightarrow \Omega_{jj'} \neq 0$$

for $j \neq j' \in \{1, \dots, p\}$ and $E(G)$ denotes the edge set of graph G . Network homogeneity problem presented in the previous paragraph can be formulated as a two-sample testing problem in statistics where we are interested in testing the null hypothesis

$$H_0 : G_1 = G_2 \tag{51}$$

In the first experiment, we use the code from Städler and Mukherjee [2019] to generate a pair of networks with 5 nodes that present 4 common edges and then obtain the corresponding correlation matrices to use as the covariance matrices for the multivariate Gaussian distribution. The results are presented in Figure 10. In the second experiment,

we again use the code from Städler and Mukherjee [2019] to generate hub networks with 7 nodes that are divided into 3 hubs with 1 hub that is different and use the obtained correlation matrices in the multivariate Gaussian distribution as with the first experiment. The results are presented in Figure 11. Both tests were able to recover the ground truth as the number of observed sample increases.

8.2 Real Data: Six-Membered Monocyclic Ring Conformation Comparison

In this section, we consider a real world application of our proposed method to detect if the conformation observed in crystal structures differ from its lowest energy conformation in gas phase. Qualitative descriptions are often given to show that the two are distributed differently due to the crystal packing effect. While no quantitative analysis has been provided in the chemistry literature, we aim to perform such analysis through the use of the proposed Bayesian two-sample test.

We utilise the Cremer-Pople puckering parameters [Cremer and Pople, 1975] to describe the six-membered monocyclic ring conformation and compare their shapes under the two different conditions described above. This coordinate system first defines a unique mean plane for a general monocyclic puckered ring. Amplitudes and Phases coordinates are then used to describe the geometry of the puckering relative to the mean plane. For a six-membered monocyclic ring, there are three puckering degrees of freedom, which are described by a single amplitude-phase pair (q_2, ϕ_2) and a single puckering coordinate q_3 . As we consider general six-membered rings, we can omit the phase parameters ϕ_2 for simplicity and compare the degree of puckering (maximal out-of-plane deviation) under different conditions. The crystal structures of 1936 six-membered monocyclic rings are extracted from the Crystallography Open Database (COD) and the associated puckering parameters are calculated. Independently, we calculate the lowest energy conformations of a diverse set of 26405 molecules using a semi-empirical method GFN2 and record the puckering parameters. We consider 100 random samples of size $n = \{200, 400, 600, 800\}$ from each of the datasets and conduct our Bayesian two-sample test 100 times while inferring the kernel

bandwidth parameter θ .

Figure 12 illustrates the results of our test. The proposed method is becoming more certain that the lowest energy conformation in gas phase of six-membered monocyclic rings is distributed differently from its crystal structures as the number of samples increases. At 800 samples, the proposed method gives the probability of $M = 1 | \mathcal{D}$ equals to 1 which aligns with expert opinions that the two are indeed distributed differently due to the crystal packing effect. In Figure 13, we provide the posterior histogram of $\theta | M = 1, \mathcal{D}$ when 800 samples are observed. The frequency distribution is multi-model indicating that multiple lengthscale is of interest for this problem at hand.

9 Conclusion

In this work, we have proposed a Bayesian two-sample testing framework utilising the Bayes factor. Rather than directly considering the observations, we have proposed to consider the differences between the empirical kernel mean embeddings (KME) evaluated at a set of inducing points. Following the learning procedure of the empirical KME [Flaxman et al., 2016], we have derived the Bayes factors when the kernel hyperparameter is given as well as when it is treated in a fully Bayesian way and marginalised over. Further, we have obtained efficient computation methods for the marginal pseudolikelihood utilising the Kronecker structure of the covariance matrices. The posterior inference of the model label and the kernel hyperparameter is done by HMC within Gibbs. We have showed in a range of synthetic and real experiments that our proposed Bayesian test is able to simultaneously utilising multiple lengthscales and correctly uncover the ground truth given sufficient data.

Following this work, there are several possible directions for future research. We have seen in Section 7 that larger sample sizes are required for more challenging problems. A random Fourier feature approximation of the above framework can be easily developed to enable the use of large sample size without having prohibitive runtime. In this case, explicit finite dimensional feature maps are available, the difference between the mean embeddings $\delta = \mu_X - \mu_Y$ can be written more explicitly as $\delta = \mathbb{E}(\phi(X)) - \mathbb{E}(\phi(Y))$. Assume a GP prior with an appropriate covariance matrix for δ , $\phi(x_i) - \phi(y_i)$ can be modelled by a Gaussian

distribution with mean $\mathbb{E}(\phi(X)) - \mathbb{E}(\phi(Y))$ and covariance estimated as presented in the Supplementary Material. While the rest of the inference procedure can follow similarly as presented here, this large scale approximation requires careful specification of the covariance matrix for the GP model of δ to ensure that draws from such GP lie in the correct RKHS.

Recently, Kamary et al. [2014] proposed a mixture modelling framework for Bayesian model selection. The proposed Bayesian two-sample testing framework using Bayes factor can be equivalently formulated as a mixture model:

$$\Delta|\theta, \pi \sim \pi N(0, \frac{1}{n}\Sigma_\theta) + (1 - \pi)N(0, R_\theta + \frac{1}{n}\Sigma_\theta).$$

The posterior distribution of the mixture proportion $0 \leq \pi \leq 1$ indicates the model preferred. A joint inference of π and the kernel bandwidth parameter θ can be easily done through MCMC. It would be interesting to see if there is a difference in performance between the mixture approach and the Bayes factor approach proposed here. Lastly, the Bayesian testing framework developed here and the directions for future work can all be applied to independence testing.

Acknowledgements

Q. Z. is supported by the Engineering and Physical Sciences Research Council (EPSRC) (EP/M50659X/1). The authors thank Lucian Chan for helping with the chemistry data and Chris Holmes whose advice in the early stages of the project was instrumental in shaping its direction.

References

- A. Ben-Israel. The Change-of-Variables Formula Using Matrix Volume. *SIAM Journal on Matrix Analysis and Applications*, 21(1):300–312, 1999.
- A. Berlinet and C. Thomas-Agnan. *Reproducing Kernel Hilbert Spaces in Probability and Statistics*. Kluwer, 2004.
- J.M. Bernardo and A.F.M. Smith. *Bayesian Theory*. Wiley, 2000.

K.M. Borgwardt and Z. Ghahramani. Bayesian Two-Sample Tests. *ArXiv e-prints: 0906.4032*, 2009.

K.M. Borgwardt, A. Gretton, M.J. Rasch, H P. Kriegel, B. Schölkopf, and A.J. Smola. Integrating Structured Biological Data by Kernel Maximum Mean Discrepancy. *Bioinformatics*, 22(14):49–57, 2006.

D. Cremer and J. A. Pople. General Definition of Ring Puckering Coordinates. *Journal of the American Chemical Society*, 97(6):1354–1358, 1975.

M.H. DeGroot. Doing What Comes Naturally: Interpreting a Tail Area as a Posterior Probability or as a Likelihood Ratio. *Journal of the American Statistical Association*, 68 (344):966–969, 1973.

S. Filippi and C.C. Holmes. A Bayesian Nonparametric Approach to Testing for Dependence Between Random Variables. *Bayesian Analysis Advance Publication*, 2016.

S. Filippi, C.C. Holmes, and L.E. Nieto-Barajas. Scalable Bayesian Nonparametric Measures for Exploring Pairwise Dependence via Dirichlet Process Mixtures. *Electronic Journal of Statistics*, 10(2):3338–3354, 2016.

S. Flaxman, D. Sejdinovic, J.P. Cunningham, and S. Filippi. Bayesian Learning of Kernel Embeddings. In *Uncertainty in Artificial Intelligence (UAI)*, pages 182–191, 2016.

K. Fukumizu, A. Gretton, X.H. Sun, and B. Schölkopf. Kernel Measures of Conditional Dependence. In *Advances in Neural Information Processing Systems (NIPS)*, 2008.

A. Gretton, K. Borgwardt, M.J. Rasch, B. Schölkopf, and A. Smola. A Kernel Two-Sample Test. *Journal of Machine Learning Research (JMLR)*, 13:723–773, 2012a.

A. Gretton, B. Sriperumbudur, D. Sejdinovic, H. Strathmann, S. Balakrishnan, M. Pontil, and K. Fukumizu. Optimal Kernel Choice for Large-Scale Two-Sample Tests. *Advances in Neural Information Processing Systems (NIPS)*, 2012b.

C.C. Holmes, F. Caron, J.E. Griffin, and D.A. Stephens. Two-Sample Bayesian Nonparametric Hypothesis Testing. *Bayesian Analysis*, 10(2):297–320, 06 2015.

W.H. Jefferys and J.O. Berger. Ockhams Razor and Bayesian Analysis. *American Journal of Science*, 80(1):64–72, 1992.

H. Jeffreys. Some Tests of Significance, Treated by the Theory of Probability. *Proceedings of the Cambridge Philosophy Society*, (31):203–222, 1935.

H. Jeffreys. *Theory of Probability*. Oxford University Press, 1961.

K. Kamary, K. Mengersen, C.P. Robert, and J. Rousseau. Testing Hypotheses via a Mixture Estimation Model. *ArXiv e-prints: 1412.2044*, 2014.

R.E. Kass and A.E. Raftery. Bayes Factors. *Journal of the American Statistical Association*, 90(430):773–795, June 1995.

M.N. Lukić and J.H. Beder. Stochastic Processes with Sample Paths in Reproducing Kernel Hilbert Spaces. *Transaction of the American Mathematical Society*, 353(10):3945–3969, 2001.

D.J.C. MacKay. *Information Theory, Inference, and Learning Algorithms*. Cambridge University Press, 2003.

J. Shawe-Taylor and N. Cristianini. *Kernel Methods for Pattern Analysis*, volume 19 of 22. Cambridge University Press, 2004.

A. Smola, A. Gretton, L. Song, and B. Schölkopf. A Hilbert Space Embedding for Distributions. In *Proceedings of the 18th International Conference on Algorithmic Learning Theory*, pages 13–31, 2007.

B.K. Sriperumbudur. Reproducing Kernel Space Embeddings and Metrics on Probability Measures. *PhD Thesis, University of California–San Diego*, 2010.

N. Städler and S. Mukherjee. TwoSample Testing in High Dimensions. *Journal of Royal Statistical Society Statistical Methodology Series B*, 79(1):225–246, 2017.

N. Städler and S. Mukherjee. A Bioconductor Package for Investigation of Network Heterogeneity From High-Dimensional Data, oct 2019. URL <https://www.bioconductor.org/packages/release/bioc/vignettes/nethet/inst/doc/nethet.pdf>.

O. Stegle, K.J. Denby, E.J. Cooke, D.L. Wild, Z. Ghahramani, and K.M. Borgwardt. A Robust Bayesian Two-Sample Test for Detecting Intervals of Differential Gene Expression in Microarray Time Series. *Journal of Computational Biology*, 17(3), 2010.

I. Steinwart and A. Christmann. *Support Vector Machines*. Springer, 2008.

G. Wahba. *Spline Models for Observational Data*. Society for Industrial and Applied Mathematics, 1990.

SUPPLEMENTARY MATERIAL

Efficient Computation of Marginal Pseudolikelihood: In this section, we illustrate the efficient computation of the multivariate Gaussian distribution utilising the Kronecker product structure of our problem. Note, Flaxman et al. [2016] used the identity matrix as Σ_θ which results in their particular derivation of the fast computation of the marginal pseudolikelihood in their section A.4. However, we propose a different approach considering the full covariance matrix Σ_θ . Recall, under the alternative hypothesis the log marginal pseudolikelihood is

$$\begin{aligned} \log p(\{(x_i, y_i)\}_{i=1}^n | \theta) &\propto -\frac{1}{2} \log \det(\mathbf{1}\mathbf{1}^\top \otimes R_\theta + I_n \otimes \Sigma_\theta) \\ &\quad - \frac{1}{2} \text{vec}(G_\theta)^\top (\mathbf{1}\mathbf{1}^\top \otimes R_\theta + I_n \otimes \Sigma_\theta)^{-1} \text{vec}(G_\theta) \\ &\quad + \frac{1}{2} \sum_{i=1}^n \log \det(J_\theta(x_i, y_i)^\top J_\theta(x_i, y_i)). \end{aligned} \quad (52)$$

We propose the efficient computation method through the following proposition.

Proposition. Denote $W_\theta := \mathbf{1}\mathbf{1}^\top \otimes R_\theta + I_n \otimes \Sigma_\theta$. Then,

$$(a) \det(W_\theta) = \det(\Sigma_\theta + nR_\theta) \det(\Sigma_\theta)^{n-1}.$$

$$(b) \text{vec}(G_\theta)^\top W_\theta^{-1} \text{vec}(G_\theta) = \text{Tr} \left((\Sigma_\theta + nR_\theta)^{-1} G_\theta G_\theta^\top + \left(\frac{1}{n} \Sigma_\theta R_\theta^{-1} \Sigma_\theta + \Sigma_\theta \right)^{-1} G_\theta H G_\theta^\top \right)$$

where $H = I - \frac{1}{n}\mathbf{1}\mathbf{1}^\top$.

Proof. (a) Using matrix determinant lemma, and note that for any $m \times m$ matrix,

$$\mathbf{1}\mathbf{1}^\top \otimes A = (\mathbf{1} \otimes I_m) A (\mathbf{1} \otimes I_m)^\top.$$

Hence, the first term of W can be written as

$$\mathbf{1}\mathbf{1}^\top \otimes R_\theta = (\mathbf{1} \otimes I_m) R_\theta (\mathbf{1} \otimes I_m)^\top.$$

For the second term of W ,

$$\det(I_n \otimes \Sigma_\theta) = \det(I_n)^m \det(\Sigma_\theta)^n = \det(\Sigma_\theta)^n$$

by the property of the determinant of Kronecker product. We can then write

$$\begin{aligned} & \det(\mathbf{1}\mathbf{1}^\top \otimes R_\theta + I_n \otimes \Sigma_\theta) \\ &= \det((\mathbf{1} \otimes I_m) R_\theta (\mathbf{1} \otimes I_m)^\top + I_n \otimes \Sigma_\theta) \\ &= \det(I + (\mathbf{1} \otimes I_m)^\top (I_n \otimes \Sigma_\theta)^{-1} (\mathbf{1} \otimes I_m) R_\theta) \det(\Sigma_\theta)^n \end{aligned} \quad (53)$$

The last equation follows from the property that $\det(A+UV^\top) = \det(I+V^\top A^{-1}U)\det(A)$ given conformable matrices. Recall the properties of Kronecker products: $(\mathbf{1} \otimes I_m)^\top = \mathbf{1}^\top \otimes I_m^\top$; $(I_n \otimes \Sigma_\theta)^{-1} = I_n^{-1} \otimes \Sigma_\theta^{-1}$ and $(A \otimes B)(C \otimes D) = (AC) \otimes (BD)$ for conformable matrices. By repetitive applications of these properties, the above can be simplified into

$$\begin{aligned} & \det(I + (\mathbf{1}^\top \otimes \Sigma_\theta^{-1})(\mathbf{1} \otimes I_m) R_\theta) \det(\Sigma_\theta)^n \\ &= \det(I + (\mathbf{1}^\top \mathbf{1}) \otimes (\Sigma_\theta^{-1} I_m) R_\theta) \det(\Sigma_\theta)^n \\ &= \det(I + n\Sigma_\theta^{-1} R_\theta) \det(\Sigma_\theta)^n \\ &= \det(\Sigma_\theta^{-1}(\Sigma_\theta + nR_\theta)) \det(\Sigma_\theta)^n \\ &= \det(\Sigma_\theta)^{-1} \det(\Sigma_\theta + nR_\theta) \det(\Sigma_\theta)^n \\ &= \det(\Sigma_\theta + nR_\theta) \det(\Sigma_\theta)^{n-1} \end{aligned}$$

Hence the desired equation is obtained.

(b) Using Woodbury identity and the properties of the Kronecker product,

$$W_\theta^{-1} = I_n \otimes \Sigma_\theta^{-1} - (\mathbf{1} \otimes \Sigma_\theta^{-1}) \left((R_\theta)^{-1} + n\Sigma_\theta^{-1} \right)^{-1} (\mathbf{1}^\top \otimes \Sigma_\theta^{-1}). \quad (54)$$

Note that $(I_n \otimes \Sigma_\theta^{-1}) \text{vec}(G_\theta) = \text{vec}(\Sigma_\theta^{-1} G_\theta)$ and

$$\{\text{vec}(G_\theta)^\top (\mathbf{1} \otimes \Sigma_\theta^{-1})\}^\top = (\mathbf{1}^\top \otimes \Sigma_\theta^{-1}) \text{vec}(G_\theta) = \text{vec}(\Sigma_\theta^{-1} G_\theta \mathbf{1}) = \Sigma_\theta^{-1} G_\theta \mathbf{1},$$

and rearranging products under the trace, we have

$$\begin{aligned} & \text{vec}(G_\theta)^\top W_\theta^{-1} \text{vec}(G_\theta) \\ &= \text{vec}(G_\theta)^\top \text{vec}(\Sigma_\theta^{-1} G_\theta) - (\Sigma_\theta^{-1} G_\theta \mathbf{1})^\top \left((R_\theta)^{-1} + n\Sigma_\theta^{-1} \right)^{-1} \Sigma_\theta^{-1} G_\theta \mathbf{1} \\ &= \text{Tr}(G_\theta^\top \Sigma_\theta^{-1} G_\theta) - \text{Tr}(\mathbf{1}^\top G_\theta^\top \Sigma_\theta^{-1} \left((R_\theta)^{-1} + n\Sigma_\theta^{-1} \right)^{-1} \Sigma_\theta^{-1} G_\theta \mathbf{1}) \\ &= \text{Tr} \left(\Sigma_\theta^{-1} G_\theta G_\theta^\top - \Sigma_\theta^{-1} \left((R_\theta)^{-1} + n\Sigma_\theta^{-1} \right)^{-1} \Sigma_\theta^{-1} G_\theta \mathbf{1} \mathbf{1}^\top G_\theta^\top \right). \end{aligned} \quad (55)$$

Denoting the matrix under the trace by A , we can further simplify

$$\begin{aligned} A &= \Sigma_\theta^{-1} G_\theta G_\theta^\top - \Sigma_\theta^{-1} \left((nR_\theta)^{-1} + \Sigma_\theta^{-1} \right)^{-1} \Sigma_\theta^{-1} G_\theta \left(\frac{1}{n} \mathbf{1} \mathbf{1}^\top \right) G_\theta^\top \\ &= \left((nR_\theta)^{-1} + \Sigma_\theta^{-1} \right) \left((nR_\theta)^{-1} + \Sigma_\theta^{-1} \right)^{-1} \Sigma_\theta^{-1} G_\theta G_\theta^\top \\ &\quad - \Sigma_\theta^{-1} \left((nR_\theta)^{-1} + \Sigma_\theta^{-1} \right)^{-1} \Sigma_\theta^{-1} G_\theta \left(\frac{1}{n} \mathbf{1} \mathbf{1}^\top \right) G_\theta^\top \\ &= (nR_\theta)^{-1} \left((nR_\theta)^{-1} + \Sigma_\theta^{-1} \right)^{-1} \Sigma_\theta^{-1} G_\theta G_\theta^\top \\ &\quad + \Sigma_\theta^{-1} \left((nR_\theta)^{-1} + \Sigma_\theta^{-1} \right)^{-1} \Sigma_\theta^{-1} G_\theta \left(I_n - \frac{1}{n} \mathbf{1} \mathbf{1}^\top \right) G_\theta^\top \\ &= (\Sigma_\theta + nR_\theta)^{-1} G_\theta G_\theta^\top + \left(\frac{1}{n} \Sigma_\theta R_\theta^{-1} \Sigma_\theta + \Sigma_\theta \right)^{-1} G_\theta H G_\theta^\top. \end{aligned}$$

Remark. The above simplifies further when $\hat{\Sigma}_\theta$ is the empirical covariance of G_θ 's,

i.e. $\hat{\Sigma}_\theta = \frac{1}{n} G_\theta H G_\theta^\top$. Indeed,

$$\begin{aligned}
& \text{Tr} \left(\left(\hat{\Sigma}_\theta + nR_\theta \right)^{-1} G_\theta G_\theta^\top + \left(\frac{1}{n} \hat{\Sigma}_\theta R_\theta^{-1} \hat{\Sigma}_\theta + \hat{\Sigma}_\theta \right)^{-1} G_\theta H G_\theta^\top \right) \\
&= \text{Tr} \left(\left(\hat{\Sigma}_\theta + nR_\theta \right)^{-1} G_\theta G_\theta^\top + \left(\hat{\Sigma}_\theta + nR_\theta \right)^{-1} nR_\theta \hat{\Sigma}_\theta^{-1} G_\theta H G_\theta^\top \right) \\
&= \text{Tr} \left(\left(\hat{\Sigma}_\theta + nR_\theta \right)^{-1} G_\theta G_\theta^\top + \left(\hat{\Sigma}_\theta + nR_\theta \right)^{-1} n^2 R_\theta \right) \\
&= \text{Tr} \left(\left(G_\theta H G_\theta^\top + n^2 R_\theta \right)^{-1} n G_\theta G_\theta^\top + \left(G_\theta H G_\theta^\top + n^2 R_\theta \right)^{-1} n^3 R_\theta \right) \\
&= \text{Tr} \left(n \left(G_\theta H G_\theta^\top + n^2 R_\theta \right)^{-1} \left(G_\theta G_\theta^\top + n^2 R_\theta \right) \right).
\end{aligned}$$

In the case of the null model, the derivation of the efficient computation of the marginal pseudolikelihood simplifies that of the alternative model. Recall, under the null hypothesis, the log marginal pseudolikelihood is

$$\begin{aligned}
& \log p(\{x_i, y_i\}_{i=1}^n | \theta) \\
& \propto -0.5 \log \det(I_n \otimes \Sigma_\theta) - 0.5 \text{vec}(G_\theta)^\top (I_n \otimes \Sigma_\theta)^{-1} \text{vec}(G_\theta) + \sum_{i=1}^n \log \text{vol}(J_\theta(x_i, y_i)).
\end{aligned} \tag{56}$$

The following lemma shows how the most costly term $\text{vec}(G_\theta)^\top (I_n \otimes \Sigma_\theta)^{-1} \text{vec}(G_\theta)$ can be computed more efficiently.

Lemma. $\text{vec}(G_\theta)^\top (I_n \otimes \Sigma_\theta)^{-1} \text{vec}(G_\theta) = \text{Tr}(G^\top \Sigma^{-1} G)$.

Proof. By properties of matrix inversion:

$$(I_n \otimes \Sigma_\theta)^{-1} = I_n^{-1} \otimes \Sigma_\theta^{-1} = I_n \otimes \Sigma_\theta^{-1}.$$

Note that $(I_n \otimes \Sigma_\theta^{-1}) \text{vec}(G) = \text{vec}(\Sigma_\theta^{-1} G)$, we have

$$\text{vec}(G)^\top (I_n \otimes \Sigma_\theta^{-1}) \text{vec}(G) = \text{vec}(G)^\top \text{vec}(\Sigma_\theta^{-1} G) = \text{Tr}(G^\top \Sigma_\theta^{-1} G).$$

Covariance Matrix Σ_θ Estimations In this section, we consider two approaches of estimating the empirical covariance matrix Σ_θ . This is common to both the null and the alternative models. It is important to note that the inducing points $\mathbf{z} = \{z_i\}_{i=1}^p$ are

treated as fixed. The first approach computes the covariance of the random variable Δ_{XY} directly and assumes independence between the random variables X and Y . The second approach, on the other hand, computes the empirical covariance matrix of $g_\theta(X, Y)$ and does not require the independence assumption.

Method 1

In this approach, we consider the covariance of the random variable Δ_{XY} . The ij^{th} component of the estimated covariance matrix $\hat{\Sigma}_{ij} = \text{Cov}([\Delta_{XY}]_i, [\Delta_{XY}]_j)$ can be written as

$$\mathbb{E}_{XY}((\hat{\mu}_X(z_i) - \hat{\mu}_Y(z_i))(\hat{\mu}_X(z_j) - \hat{\mu}_Y(z_j))) \quad (57)$$

$$= \mathbb{E}_{XY}(\hat{\mu}_X(z_i)\hat{\mu}_X(z_j) - \hat{\mu}_X(z_i)\hat{\mu}_Y(z_j) + \hat{\mu}_Y(z_i)\hat{\mu}_Y(z_j) - \hat{\mu}_Y(z_i)\hat{\mu}_X(z_j)). \quad (58)$$

The first term of (58) can be expanded as

$$\mathbb{E}_X(\hat{\mu}_X(z_i)\hat{\mu}_X(z_j)) \quad (59)$$

$$= \mathbb{E}_X\left(\frac{1}{n^2} \sum_{a=1}^n \sum_{b=1}^n k(X_a, z_i)k(X_b, z_j)\right) \quad (60)$$

$$= \frac{1}{n^2} \left[\sum_{a=1}^n \mathbb{E}_X(k(X_a, z_i)k(X_a, z_j)) + \sum_{b=1}^n \sum_{b \neq a} \mathbb{E}_X(k(X_a, z_i)k(X_b, z_j)) \right] \quad (61)$$

$$= \frac{1}{n^2} [n\mathbb{E}_X(k(X, z_i)k(X, z_j)) + n(n-1)\mathbb{E}_X(k(X, z_i)k(X, z_j))] \quad (62)$$

Given observations $\{(x_i, y_i)\}_{i=1}^n$, the above is now readily estimated as

$$\approx \frac{1}{n^2} \sum_{a=1}^n k(x_a, z_i)k(x_a, z_j) + \frac{n-1}{n} \left(\frac{1}{n} \sum_{a=1}^n k(x_a, z_i) \right) \left(\frac{1}{n} \sum_{b=1}^n k(x_b, z_j) \right) \quad (63)$$

$$= \frac{1}{n^2} K_{z_i \mathbf{x}} K_{\mathbf{x} z_j} + \frac{n-1}{n} \left(\frac{1}{n} K_{z_i \mathbf{x}} \mathbb{1} \right) \left(\frac{1}{n} K_{z_j \mathbf{x}} \mathbb{1} \right) \quad (64)$$

$$= \frac{1}{n^2} K_{z_i \mathbf{x}} K_{\mathbf{x} z_j} + \frac{n-1}{n} \hat{\mu}_x(z_i)\hat{\mu}_x(z_j), \quad (65)$$

where $\mathbb{1}$ is a vector of 1s in \mathbb{R}^n and $\mathbf{x} = [x_1 \cdots x_n]^\top \in \mathbb{R}^{n \times D}$. Similarly, the third term in (58) can be approximated as

$$\mathbb{E}_Y(\hat{\mu}_Y(z_i)\hat{\mu}_Y(z_j)) \approx \frac{1}{n^2} K_{z_i \mathbf{y}} K_{\mathbf{y} z_j} + \frac{n-1}{n} (\hat{\mu}_y(z_i))(\hat{\mu}_y(z_j)) \quad (66)$$

where $\mathbf{y} = [y_1 \cdots y_n]^\top \in \mathbb{R}^{n \times D}$. Assuming that X and Y are independent, the second term in (58) can be empirically estimated as

$$\mathbb{E}_{XY}(\hat{\mu}_X(z_i)\hat{\mu}_Y(z_j)) \quad (67)$$

$$= \left(\frac{1}{n} \sum_{a=1}^n \mathbb{E}_X(k(X_a, z_i)) \right) \left(\frac{1}{n} \sum_{b=1}^n \mathbb{E}_Y(k(Y_b, z_j)) \right) \quad (68)$$

$$\approx (\hat{\mu}_x(z_i))(\hat{\mu}_y(z_j)) \quad (69)$$

and similarly for the fourth term of (58). When we consider all $\mathbf{z} = \{z_1, \dots, z_p\}$, (58) can be written as

$$\mathbb{E}_{XY}((\hat{\mu}_X(\mathbf{z}) - \hat{\mu}_Y(\mathbf{z}))(\hat{\mu}_X(\mathbf{z}) - \hat{\mu}_Y(\mathbf{z}))^\top) \quad (70)$$

$$\begin{aligned} &\approx \frac{1}{n^2} K_{\mathbf{zx}} K_{\mathbf{xz}} + \frac{n-1}{n} \hat{\mu}_x(\mathbf{z}) \hat{\mu}_x(\mathbf{z})^\top - \hat{\mu}_x(\mathbf{z}) \hat{\mu}_y(\mathbf{z})^\top \\ &\quad + \frac{1}{n^2} K_{\mathbf{zy}} K_{\mathbf{yz}} + \frac{n-1}{n} \hat{\mu}_y(\mathbf{z}) \hat{\mu}_y(\mathbf{z})^\top - \hat{\mu}_y(\mathbf{z}) \hat{\mu}_x(\mathbf{z})^\top. \end{aligned} \quad (71)$$

The second term of $\hat{\Sigma} = \text{Cov}(\Delta_{XY})$ can be written as

$$[\mathbb{E}_{XY}(\hat{\mu}_X(\mathbf{z}) - \hat{\mu}_Y(\mathbf{z}))][\mathbb{E}(\hat{\mu}_X(\mathbf{z}) - \hat{\mu}_Y(\mathbf{z}))]^\top \quad (72)$$

$$\approx \hat{\mu}_x(\mathbf{z}) \hat{\mu}_x(\mathbf{z})^\top + \hat{\mu}_y(\mathbf{z}) \hat{\mu}_y(\mathbf{z})^\top - \hat{\mu}_x(\mathbf{z}) \hat{\mu}_y(\mathbf{z})^\top - \hat{\mu}_y(\mathbf{z}) \hat{\mu}_x(\mathbf{z})^\top \quad (73)$$

Overall the empirical estimate of $\hat{\Sigma}$ can be computed as

$$\text{Cov}(\Delta_{XY}) \quad (74)$$

$$\begin{aligned} &= \mathbb{E}_{XY}((\hat{\mu}_X(\mathbf{z}) - \hat{\mu}_Y(\mathbf{z}))(\hat{\mu}_X(\mathbf{z}) - \hat{\mu}_Y(\mathbf{z}))^\top) \\ &\quad - \mathbb{E}(\hat{\mu}_X(\mathbf{z}) - \hat{\mu}_Y(\mathbf{z})) \mathbb{E}(\hat{\mu}_X(\mathbf{z}) - \hat{\mu}_Y(\mathbf{z}))^\top \end{aligned} \quad (75)$$

$$\approx \frac{1}{n^2} K_{\mathbf{zx}} K_{\mathbf{xz}} - \frac{1}{n} \hat{\mu}_x(\mathbf{z}) \hat{\mu}_x(\mathbf{z})^\top + \frac{1}{n^2} K_{\mathbf{zy}} K_{\mathbf{yz}} - \frac{1}{n} \hat{\mu}_y(\mathbf{z}) \hat{\mu}_y(\mathbf{z})^\top \quad (76)$$

$$= \frac{1}{n^2} K_{\mathbf{zx}} H K_{\mathbf{xz}} + \frac{1}{n^2} K_{\mathbf{zy}} H K_{\mathbf{yz}} \quad (77)$$

Since $\hat{\mu}_x(z) \hat{\mu}_x(z)^\top = \frac{1}{n^2} K_{\mathbf{zx}} \mathbb{1} \mathbb{1}^\top K_{\mathbf{xz}}$ and $H := I - \frac{1}{n} \mathbb{1} \mathbb{1}^\top$, the final estimation equation (77) follows.

Method 2

In this approach, we consider the random variable

$$g_\theta(X, Y) = (k(X, z_1) - k(Y, z_1), \dots, k(X, z_p) - k(Y, z_p))^\top.$$

The ij^{th} component of the empirical covariance matrix of $g_\theta(X, Y)$ can be written as

$$Cov(k(X, z_i) - k(Y, z_i), k(X, z_j) - k(Y, z_j)) \quad (78)$$

$$\begin{aligned} &= \mathbb{E}_{XY}((k(X, z_i) - k(Y, z_i))(k(X, z_j) - k(Y, z_j))) \\ &\quad - \mathbb{E}_{XY}((k(X, z_i) - k(Y, z_i)))\mathbb{E}_{XY}((k(X, z_j) - k(Y, z_j))) \end{aligned} \quad (79)$$

The first term of (79) can be written as

$$\mathbb{E}_{XY}((k(X, z_i) - k(Y, z_i))(k(X, z_j) - k(Y, z_j))) \quad (80)$$

$$\begin{aligned} &= \mathbb{E}_{XY}(k(X, z_i)k(X, z_j) - k(X, z_i)k(Y, z_j) - k(Y, z_i)k(X, z_j) + k(Y, z_i)k(Y, z_j)) \\ &\quad (81) \end{aligned}$$

$$\approx \frac{1}{n}K_{z_i\mathbf{x}}K_{\mathbf{x}z_j} - \frac{1}{n}K_{z_i\mathbf{x}}K_{\mathbf{y}z_j} - \frac{1}{n}K_{z_j\mathbf{x}}K_{\mathbf{y}z_i} + \frac{1}{n}K_{z_i\mathbf{y}}K_{\mathbf{y}z_j} \quad (82)$$

While the second term of (79) can be written as

$$\mathbb{E}_{XY}(k(X, z_i) - k(Y, z_i))\mathbb{E}_{XY}(k(X, z_j) - k(Y, z_j)) \quad (83)$$

$$= (\mu_X(z_i) - \mu_Y(z_i))(\mu_X(z_j) - \mu_Y(z_j)) \quad (84)$$

$$\approx \frac{1}{n^2}K_{z_i\mathbf{x}}\mathbb{1}\mathbb{1}^\top K_{\mathbf{x}z_j} - \frac{1}{n^2}K_{z_i\mathbf{x}}\mathbb{1}\mathbb{1}^\top K_{\mathbf{y}z_j} - \frac{1}{n^2}K_{z_i\mathbf{y}}\mathbb{1}\mathbb{1}^\top K_{\mathbf{x}z_i} + \frac{1}{n^2}K_{z_i\mathbf{y}}\mathbb{1}\mathbb{1}^\top K_{\mathbf{y}z_j} \quad (85)$$

Hence, combining these two terms and consider all $\mathbf{z} = \{z_1, \dots, z_p\}$:

$$Cov(g_\theta(X, Y)) \quad (86)$$

$$\approx \frac{1}{n}K_{\mathbf{z}\mathbf{x}}HK_{\mathbf{x}\mathbf{z}} + \frac{1}{n}K_{\mathbf{z}\mathbf{y}}HK_{\mathbf{y}\mathbf{z}} - \frac{1}{n}K_{\mathbf{z}\mathbf{x}}HK_{\mathbf{y}\mathbf{z}} - \frac{1}{n}K_{\mathbf{z}\mathbf{y}}HK_{\mathbf{x}\mathbf{z}} \quad (87)$$

$$= \frac{1}{n}G_\theta HG_\theta^\top. \quad (88)$$

To see how (88) follows, recall $G_\theta := [g_\theta(x_1, y_1), \dots, g_\theta(x_n, y_n)] \in \mathbb{R}^{p \times n}$ which can be equivalently written in terms of kernel matrices as $G_\theta = K_{\mathbf{z}\mathbf{x}} - K_{\mathbf{z}\mathbf{y}}$.

Note that the distribution of $g_\theta(x_i, y_i)$ arises from the distribution of Δ due to Cramer's decomposition theorem, this implies $Cov(\Delta_{XY}) = \frac{1}{n}Cov(g_\theta(X, Y))$. If in addition, we assume the independence between X and Y , the computation of $Cov(g_\theta(X, Y))$ will be simplified and the cross terms in (87) will be zero. However,

even in the case where independence assumption is satisfied, numerical instability leads to slight difference of the covariance computation between the two estimation methods. Nonetheless, we did not observe any difference of the resulting posterior inference in that case.

Computation of the Jacobian Matrix In this section, we detail the computation of the Jacobian term. As the variable under consideration is the same for the null and the alternative models, the Jacobian term remains the same. The variables under consideration is

$$g_\theta : (x, y) \mapsto (k_\theta(x, z_1) - k_\theta(y, z_1), \dots, k_\theta(x, z_p) - k_\theta(y, z_p))$$

where $g_\theta : \mathbb{R}^{2D} \rightarrow \mathbb{R}^p$. For each $i = 1, \dots, n$, the Jacobian matrix $J_\theta(x_i, y_i) \in \mathbb{R}^{p \times 2D}$:

$$J_\theta(x_i, y_i) = \left[\begin{array}{c|c} J_x(x_i) & J_y(y_i) \end{array} \right]$$

where $J_x(x_i) \in \mathbb{R}^{p \times D}$ and $J_y(y_i) \in \mathbb{R}^{p \times D}$ are block matrices separating the terms related to X and those that are related to Y. The θ dependence is omitted here for notational simplicity. $J_x(x_i)$ can be written as

$$J_x(x_i) = \left[\begin{array}{ccc} \frac{\partial}{\partial x_{.1}} g_\theta(x_i, y_i)_1 & \cdots & \frac{\partial}{\partial x_{.D}} g_\theta(x_i, y_i)_1 \\ \vdots & \ddots & \vdots \\ \frac{\partial}{\partial x_{.1}} g_\theta(x_i, y_i)_p & \cdots & \frac{\partial}{\partial x_{.D}} g_\theta(x_i, y_i)_p \end{array} \right] \quad (89)$$

and $J_y(y_i)$ can be written as

$$J_y(y_i) = \left[\begin{array}{ccc} \frac{\partial}{\partial y_{.1}} g_\theta(x_i, y_i)_1 & \cdots & \frac{\partial}{\partial y_{.D}} g_\theta(x_i, y_i)_1 \\ \vdots & \ddots & \vdots \\ \frac{\partial}{\partial y_{.1}} g_\theta(x_i, y_i)_p & \cdots & \frac{\partial}{\partial y_{.D}} g_\theta(x_i, y_i)_p \end{array} \right] \quad (90)$$

where $g_\theta(x_i, y_i)_l$ denotes the l^{th} component of $g_\theta(x_i, y_i)$, i.e. $g_\theta(x_i, y_i)_l = k_\theta(x_i, z_l) - k_\theta(y_i, z_l)$ and $\frac{\partial}{\partial x_{.d}}$ is the partial derivative with respect to the d^{th} dimension of the random variable x .

For observations of D dimension, the Gaussian RBF kernel under consideration is of the form:

$$k_\theta(x_i, z_l) = \exp\left(-\frac{1}{2\theta^2}\|x_i - z_l\|_2^2\right) \quad (91)$$

$$= \exp\left(-\frac{1}{2\theta^2} [(x_{i1} - z_{l1})^2 + \dots + (x_{iD} - z_{lD})^2]\right) \quad (92)$$

Let the Gram matrix between $\{x_i\}_{i=1}^n$ and $\{z_j\}_{j=1}^p$ be K_{xz} such that $[K_{xz}]_{il} = k_\theta(x_i, z_l)$. Similarly, $[K_{yz}]_{il} = k_\theta(y_i, z_l)$.

For each dimension $d = 1, \dots, D$, we denote the difference between x_{id} and z_{jd} for $i = 1, \dots, n$ and $j = 1, \dots, p$ as $D_d^x \in \mathbb{R}^{n \times p}$:

$$D_d^x = \begin{bmatrix} x_{1d} - z_{1d} & \dots & x_{1d} - z_{pd} \\ & \vdots & \\ x_{nd} - z_{1d} & \dots & x_{nd} - z_{pd} \end{bmatrix}. \quad (93)$$

Similarly, we have D_d^y for $d = 1, \dots, D$.

Given the form of the kernel function, each term in (89) can be written as

$$[J_x(x_i)]_{lm} = \frac{\partial g_\theta(x_i, y_i)_l}{\partial x_{\cdot m}} = \frac{\partial k_\theta(x_i, z_l)}{\partial x_{\cdot m}} \quad (94)$$

$$= \exp\left(-\frac{1}{2\theta^2} [(x_{i1} - z_{l1})^2 + \dots + (x_{iD} - z_{lD})^2]\right) \left(-\frac{2}{2\theta^2}(x_{im} - z_{lm})\right) \quad (95)$$

$$= k_\theta(x_i, z_l) \left(-\frac{1}{\theta^2}(x_{im} - z_{lm})\right) \quad (96)$$

Similarly for the Jacobian term associated with Y :

$$[J_y(y_i)]_{lm} = \frac{\partial g_\theta(x_i, y_i)_l}{\partial y_{\cdot m}} = -\frac{\partial k_\theta(y_i, z_l)}{\partial y_{\cdot m}}.$$

In computing the probability of the observations $\{x_i, y_i\}_{i=1}^n$ given the hyperparameter θ , we are interested in computing the log determinant of the Jacobian term $\log \det(J_\theta(x_i, y_i)^\top J_\theta(x_i, y_i))$.

Note, for a fixed i , the square matrix can be written as

$$J_\theta(x_i, y_i)^\top J_\theta(x_i, y_i) = \left[\begin{array}{c|c} J_x(x_i)^\top J_x(x_i) & J_x(x_i)^\top J_y(y_i) \\ \hline J_y(y_i)^\top J_x(x_i) & J_y(y_i)^\top J_y(y_i) \end{array} \right] \quad (97)$$

where each $J(\cdot_i)^\top J(\cdot_i)$ is a block matrix of dimension $D \times D$. For notational convenient, we will omit the θ in the kernel function $k_\theta(\cdot, \cdot)$ when the context is clear.

$$J_x(x_i)^\top J_x(x_i) = \left[\begin{array}{ccc} \sum_{j=1}^p \frac{\partial k(x_i, z_j)}{\partial x_{\cdot 1}} \frac{\partial k(x_i, z_j)}{\partial x_{\cdot 1}} & \cdots & \sum_{j=1}^p \frac{\partial k(x_i, z_j)}{\partial x_{\cdot 1}} \frac{\partial k(x_i, z_j)}{\partial x_{\cdot D}} \\ & \vdots & \\ \sum_{j=1}^p \frac{\partial k(x_i, z_j)}{\partial x_{\cdot D}} \frac{\partial k(x_i, z_j)}{\partial x_{\cdot 1}} & \cdots & \sum_{j=1}^p \frac{\partial k(x_i, z_j)}{\partial x_{\cdot D}} \frac{\partial k(x_i, z_j)}{\partial x_{\cdot D}} \end{array} \right] \quad (98)$$

The term $J_y(y_i)^\top J_y(y_i)$ is similar, while the cross-term can be computed as

$$J_x(x_i)^\top J_y(y_i) = \left[\begin{array}{ccc} -\sum_{j=1}^p \frac{\partial k(x_i, z_j)}{\partial x_{\cdot 1}} \frac{\partial k(y_i, z_j)}{\partial y_{\cdot 1}} & \cdots & -\sum_{j=1}^p \frac{\partial k(x_i, z_j)}{\partial x_{\cdot 1}} \frac{\partial k(y_i, z_j)}{\partial y_{\cdot D}} \\ & \vdots & \\ -\sum_{j=1}^p \frac{\partial k(x_i, z_j)}{\partial x_{\cdot D}} \frac{\partial k(y_i, z_j)}{\partial y_{\cdot 1}} & \cdots & -\sum_{j=1}^p \frac{\partial k(x_i, z_j)}{\partial x_{\cdot D}} \frac{\partial k(y_i, z_j)}{\partial y_{\cdot D}} \end{array} \right] \quad (99)$$

with

$$\begin{aligned} & [J_x(x_i)^\top J_x(x_i)]_{st} \\ &= \sum_{j=1}^p \frac{\partial k(x_i, z_j)}{\partial x_{\cdot s}} \frac{\partial k(x_i, z_j)}{\partial x_{\cdot t}} \end{aligned} \quad (100)$$

$$= \sum_{j=1}^p k_\theta(x_i, z_j) \left(-\frac{1}{\theta^2} (x_{is} - z_{js}) \right) k_\theta(x_i, z_j) \left(-\frac{1}{\theta^2} (x_{it} - z_{jt}) \right) \quad (101)$$

$$= \sum_{j=1}^p \frac{1}{\theta^4} k_\theta(x_i, z_j)^2 (x_{is} - z_{js})(x_{it} - z_{jt}) \quad (102)$$

$$= \sum_{j=1}^p \frac{1}{\theta^4} [K_{xz}]_{ij}^2 [D_s^x]_{ij} [D_t^x]_{ij}. \quad (103)$$

Essentially, the above equation indicates that we compute the row sum of the elements-wise product of these three matrices of interest. Similarly,

$$[J_x(x_i)^\top J_y(y_i)]_{st} = - \sum_{j=1}^p \frac{\partial k(x_i, z_j)}{\partial x_{\cdot s}} \frac{\partial k(y_i, z_j)}{\partial y_{\cdot t}} \quad (104)$$

$$= - \sum_{j=1}^p \frac{1}{\theta^4} [K_{xz}]_{ij} [K_{yz}]_{ij} [D_s^x]_{ij} [D_t^y]_{ij} \quad (105)$$

Equations (103) and (105) enable the computation of the square matrix $J_\theta(x_i, y_i)^\top J_\theta(x_i, y_i)$ for each $i = 1, \dots, n$.

Bayes Factor with Fixed θ Given the framework set out before and assume equal prior probabilities for the null and alternative model, when the lengthscale parameter θ is fixed, the Bayes factor can be computed directly by utilizing Gaussian distributions of Δ as

$$BF = \frac{P(\Delta|M = 0, \theta)}{P(\Delta|M = 1, \theta)} \quad (106)$$

$$\Delta|M = 0, \theta \sim N(0, \frac{1}{n}\Sigma_\theta) \quad (107)$$

$$\Delta|M = 1, \theta \sim N(0, R_\theta + \frac{1}{n}\Sigma_\theta). \quad (108)$$

We consider some simple one dimensional experiments where under the null, both samples come from $N(0, 1)$ and under the alternative, the data sample $\{y_i\}_{i=1}^n$ comes from distributions listed in Table 2.

In this experiment, we fix the θ parameter to the median heuristic. The results shown in Table 2 were obtained using 500 samples with 40 evaluation points and averaged across 100 simulations. Equivalently, by the relationship between the posterior probability of $M|\Delta = 0$ and the BF, the model clearly recovers the ground truth for distinguishing Gaussian distributions that differ in mean or variance. On the other hand, when comparing the null distribution with Laplace distributions, the model is struggling to detect the difference at 500 samples. However, when we set θ by searching over a grid of 60 values in $[0.01, 40]$ that minimises the Bayes factor, the proposed method is able to do better as presented in Table 3. Although in the case of comparing $N(0, 1)$ against $Laplace(0, \sqrt{1/2})$ (i.e. a Laplace distribution with mean 0 and variance 1) at 500 samples, the model still prefers the null hypothesis, we do observe that the value of the Bayes factor is orders of magnitude smaller. On the other hand, when comparing $N(0, 1)$ with $Laplace(0, 1.5)$ and $Laplace(0, 0.4)$, we see that the model is more certain that the two distributions are different. This highlights the fact that median heuristic is not the best method to select the lengthscale parameter for this hypothesis testing problem. In what follows, we will present a Bayesian

Alternative Model	Bayes Factor	$P(M = 0 \Delta, \theta)$
$\mathcal{N}(0, 1)$	1.79×10^{25}	1.00
$\mathcal{N}(0, 2^2)$	5.44×10^{-5}	5.44×10^{-5}
$\mathcal{N}(0, 3^2)$	2.12×10^{-51}	2.12×10^{-51}
$\mathcal{N}(1, 1)$	2.31×10^{-13}	2.31×10^{-13}
$\mathcal{N}(2, 1)$	3.55×10^{-185}	3.55×10^{-185}
$\mathcal{N}(3, 1)$	0	0
$Laplace(0, \sqrt{1/2})$	5.86×10^{22}	1.00
$Laplace(0, 1.5)$	2.13×10^7	9.99×10^{-1}
$Laplace(0, 0.4)$	6.51×10^{-2}	6.11×10^{-2}

Table 2: Table of Bayes factors and posterior probability of the null hypothesis. Recall a Bayes factor with a value greater than 1 is supporting the null hypothesis while a value smaller than 1 is supporting the alternative hypothesis. The larger the value of the Bayes factor the stronger the support for the null. Results obtained using 500 samples with 40 evaluation points and averaged across 100 simulations.

approach that infers the posterior distribution of θ and hence alleviate the need to choose a fixed lengthscale parameter whose value is crucial for the performance of our test.

Alternative Model	Bayes Factor	$P(M = 0 \Delta, \theta)$	θ
$Laplace(0, \sqrt{1/2})$	4.64×10^{13}	1.00	31.19
$Laplace(0, 1.5)$	2.13×10^{-2}	2.13×10^{-2}	4.75
$Laplace(0, 0.4)$	3.12×10^{-7}	3.12×10^{-7}	2.04

Table 3: Table of Bayes factors with θ obtained by grid search 60 values over $[0.001, 40]$.

1-Dimensional Mixture of Gaussian Distributions We have seen that the proposed Bayesian two-sample testing method works well in distinguishing 1 and 2 dimensional Gaussian distributions. In this section, we provide an additional experiment where we consider 1-dimensional mixture of Gaussian distributions as our null and alternative

models. More specifically, we consider the following list of null and alternative models where Figure 20 provides illustration of samples from these models.

- Null Model: $X \sim 0.5\mathcal{N}(0, 1) + 0.5\mathcal{N}(4, 1)$
- Alternative Model: $Y \sim 0.5\mathcal{N}(0, 4) + 0.5\mathcal{N}(4, 4)$
- Alternative Model: $Y \sim 0.5\mathcal{N}(0, 1) + 0.5\mathcal{N}(8, 1)$
- Alternative Model: $Y \sim 0.5\mathcal{N}(0, 4) + 0.5\mathcal{N}(8, 4)$
- Alternative Model: $Y \sim 0.5\mathcal{N}(2, 1) + 0.5\mathcal{N}(6, 1)$
- Alternative Model: $Y \sim 0.5\mathcal{N}(2, 4) + 0.5\mathcal{N}(8, 4)$
- Alternative Model: $Y \sim 0.5\mathcal{N}(-4, 1) + 0.5\mathcal{N}(8, 1)$
- Alternative Model: $Y \sim 0.5\mathcal{N}(-4, 4) + 0.5\mathcal{N}(8, 4)$.

For each of the models, Figure 14 and 15 show the distribution of $M = 1|\mathcal{D}$ as a function of the number of samples n . For the first plot of Figure 14, we observe that the probability consistently equals to zero for all sample sizes and for all simulated datasets. This is reassuring as the data X and Y are indeed simulated from the same distribution, i.e. we are under the null hypothesis. When the alternative model is $Y \sim 0.5\mathcal{N}(0, 4) + 0.5\mathcal{N}(4, 4)$, the problem is more challenging. At 800 samples, the test is uncertain, but preferring the null hypothesis. This comes back to the aforementioned idea of Bayesian modelling naturally prefers simple hypothesis. In the other plots of Figure 14 and 15, we observed that the distribution of $M = 1|\mathcal{D}$ gradually concentrates around 1 as the number of samples increases. This aligns with our expectations.

Additional Figures

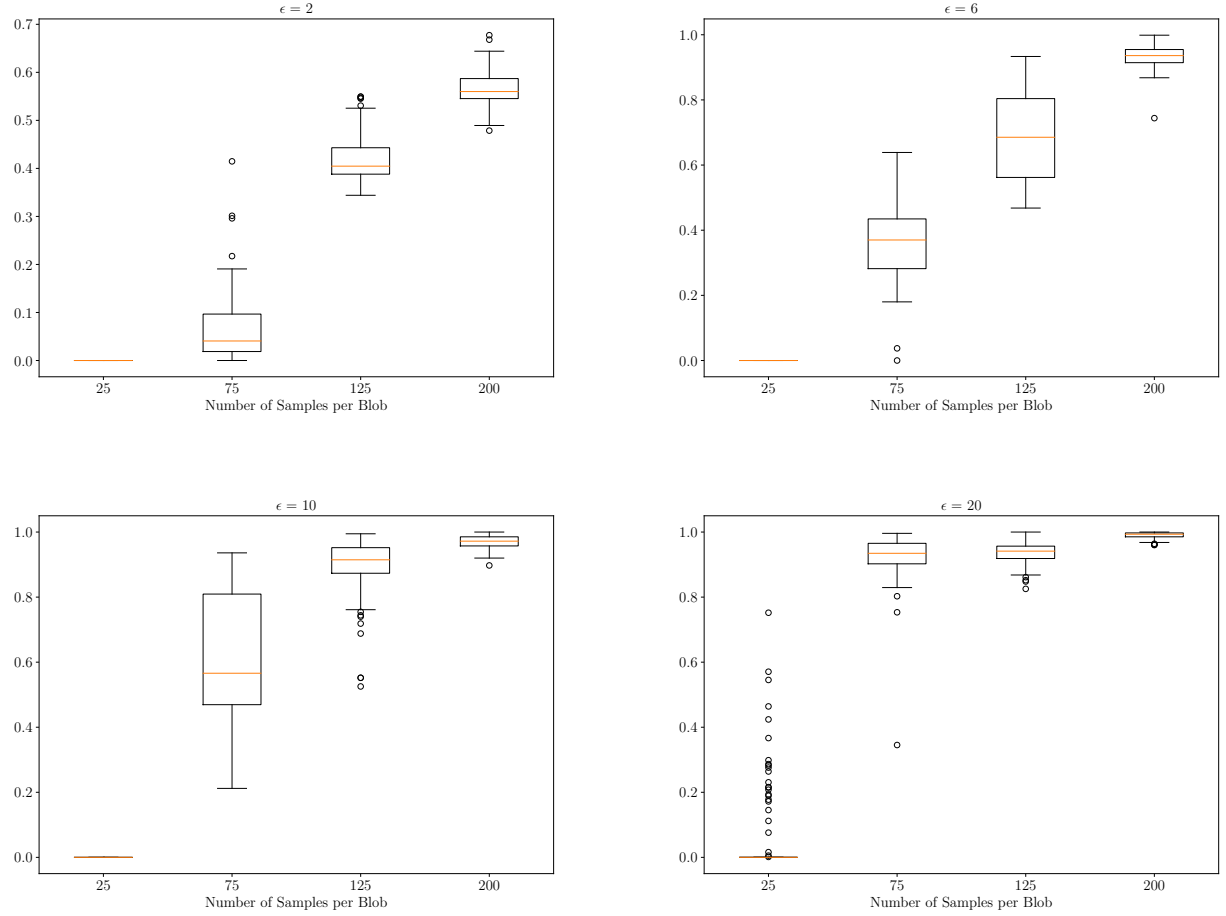


Figure 6: 2 by 2 blobs of bivariate Gaussian experiment: distribution (over 100 independent runs) of the probability of the alternative hypothesis $p(M = 1 | \mathcal{D})$ for a different number of observations n . For the distribution of X , we a mixture of four bivariate Gaussian distributions with equal probability centered at $\{(10, 10)^\top, (10, 30)^\top, (30, 10)^\top, (30, 30)^\top\}$ and with $\epsilon = 1$ as in the set up from Section 7.2. The distribution of Y is also a mixture of four bivariate Gaussian distributions with equal probability centered around the same locations but also shifted by $(-1, -1)$. In this experiment, we consider the cases when $\epsilon = \{2, 6, 10, 20\}$.

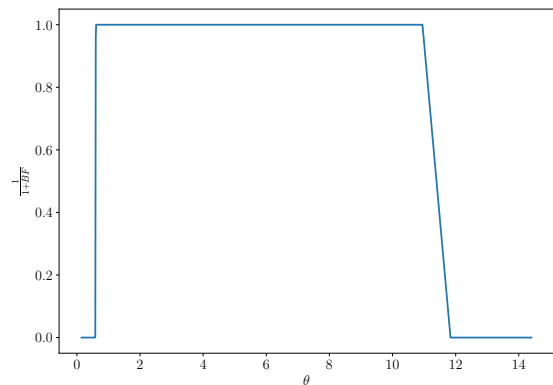


Figure 7: 2 by 2 blobs of bivariate Gaussian experiment with the alternative model $\epsilon = 2$ and 200 samples per blob. The plot illustrates $\frac{1}{1+BF_\theta}$ against the value of θ .

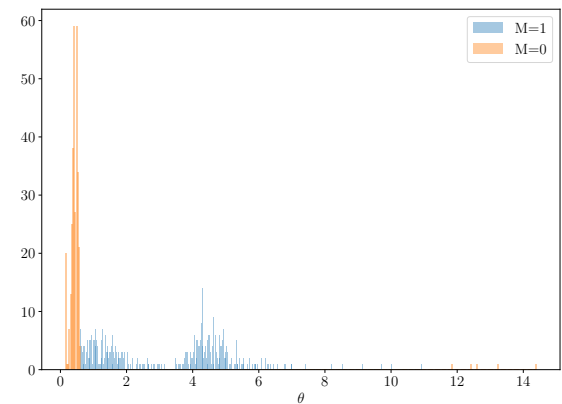


Figure 8: 2 by 2 blobs of bivariate Gaussian experiment with the alternative model $\epsilon = 2$ and 200 samples per blob. Histogram of samples from the marginal distribution of $\theta|M, \mathcal{D}$ for $M = 1$ and $M = 0$.

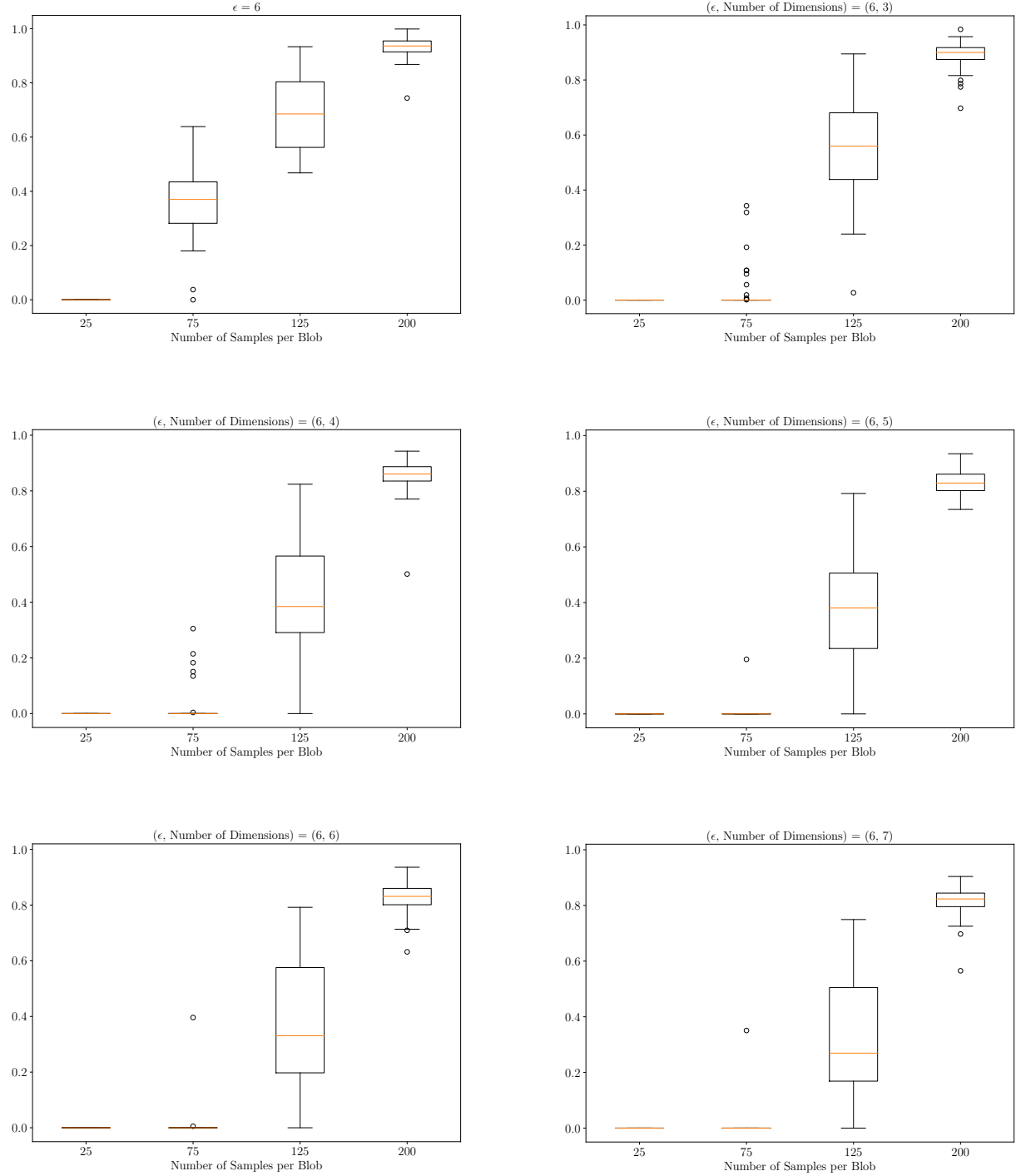


Figure 9: Higher dimensional experiment: distribution (over 100 independent runs) of the probability of the alternative hypothesis $p(M = 1|\mathcal{D})$ for a different number of observations n . For the first two dimensions, the data is generated as in Section 7.3 with $\epsilon = 6$. Standard Gaussian noises are appended as the remaining dimensions. Top left figure is copied from Figure 6 for the ease of performance comparison.

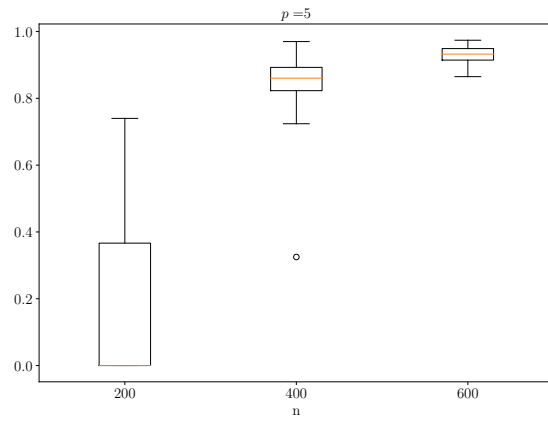


Figure 10: Random networks heterogeneity testing: distribution (over 100 independent runs) of the probability of $M = 1|\mathcal{D}$ for a different number of samples.

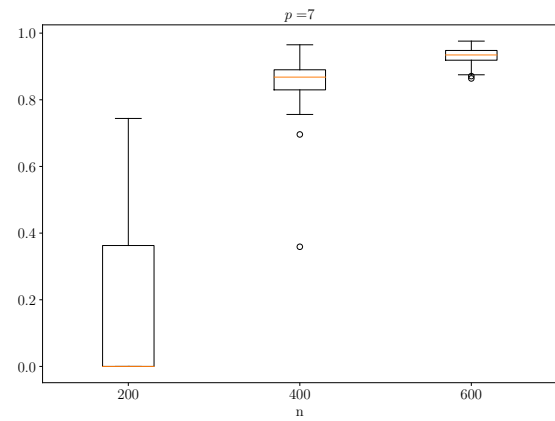


Figure 11: Hub network heterogeneity testing: distribution (over 100 independent runs) of the probability of $M = 1|\mathcal{D}$ for a different number of samples.

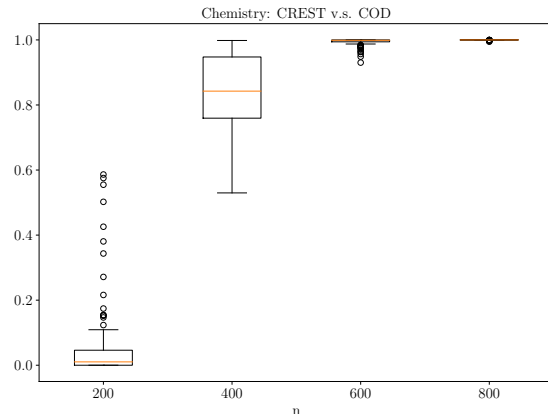


Figure 12: Six-membered monocyclic ring conformation comparison: distribution (over 100 independent runs) of the probability of $M = 1|\mathcal{D}$ for a different number of samples.

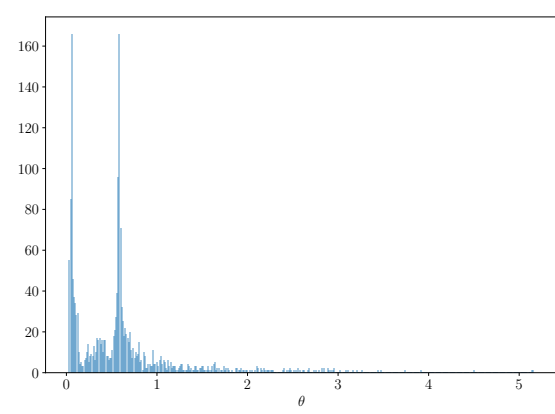


Figure 13: Histogram of samples from the marginal distribution $\theta|M = 1, \mathcal{D}$ for the experiment on six-membered monocyclic ring conformation comparison with 800 samples.

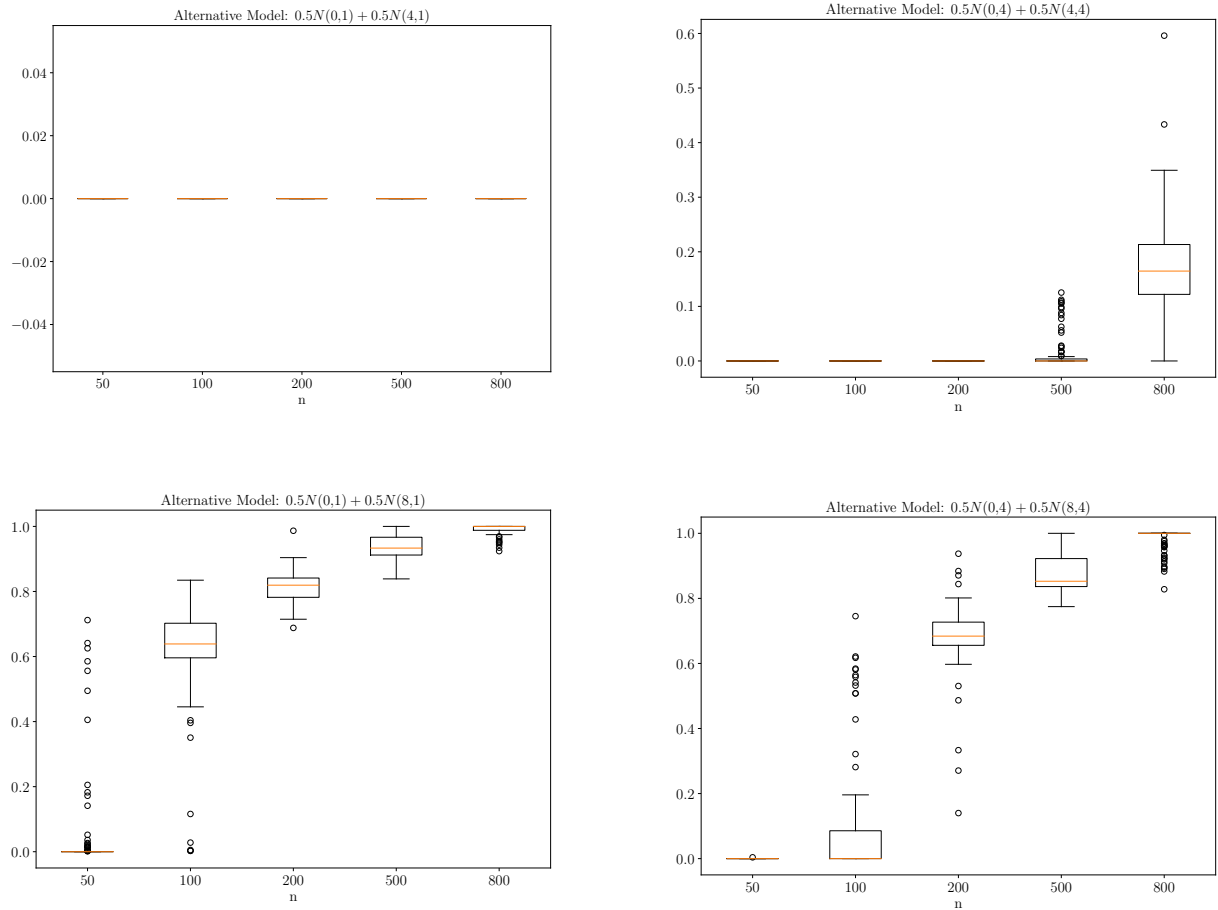


Figure 14: 1-dimensional mixture of Gaussian distributions: distribution (over 100 independent runs) of the probability of the alternative hypothesis $p(M = 1 | \mathcal{D})$ for a different number of observations n . The null model is $X \stackrel{i.i.d.}{\sim} 0.5\mathcal{N}(0, 1) + 0.5\mathcal{N}(4, 1)$ and the alternative model is presented as the title of each plot. Continue onto the next page.

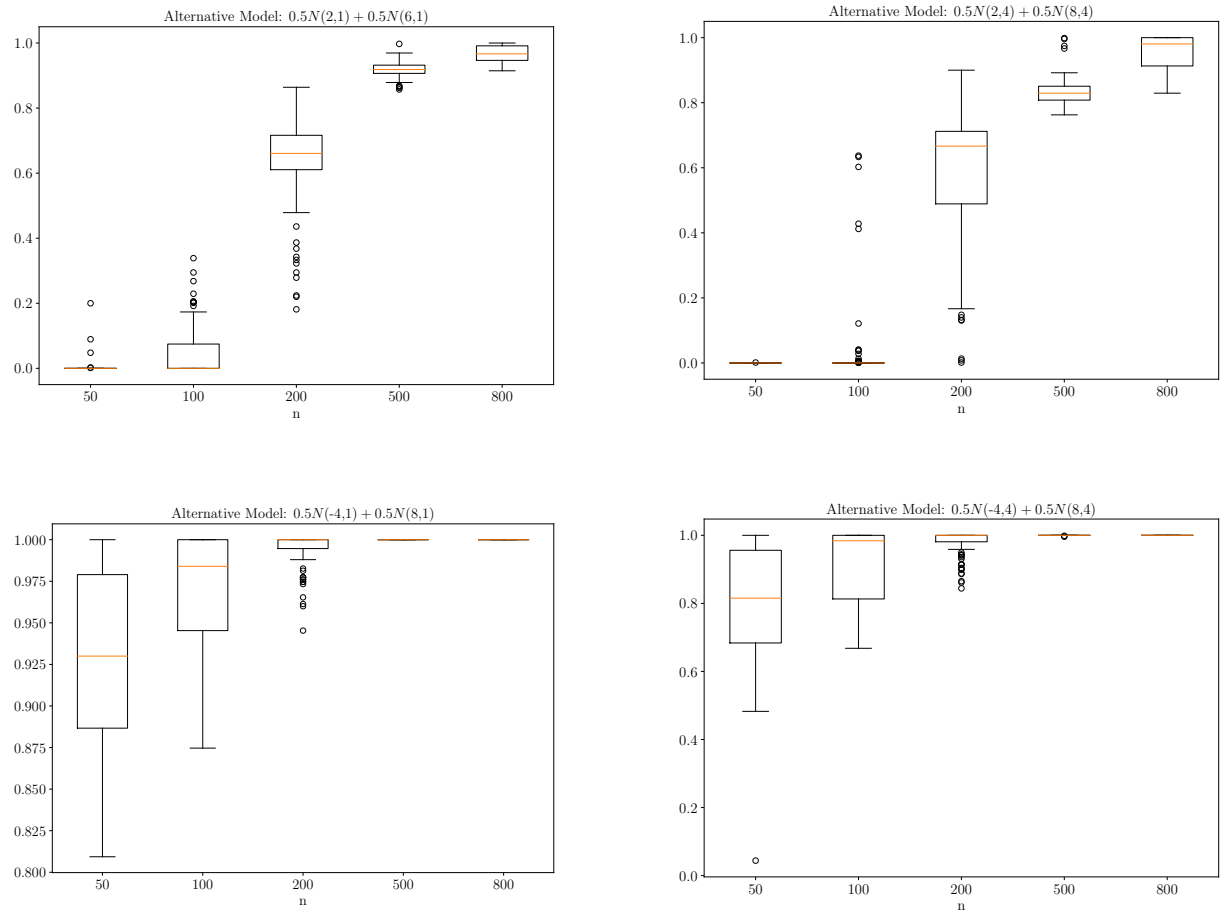


Figure 15: 1-dimensional mixture of Gaussian distributions: distribution (over 100 independent runs) of the probability of the alternative hypothesis $p(M = 1 | \mathcal{D})$ for a different number of observations n . The null model is $X \stackrel{i.i.d.}{\sim} 0.5\mathcal{N}(0, 1) + 0.5\mathcal{N}(4, 1)$ and the alternative model is presented as the title of each plot.

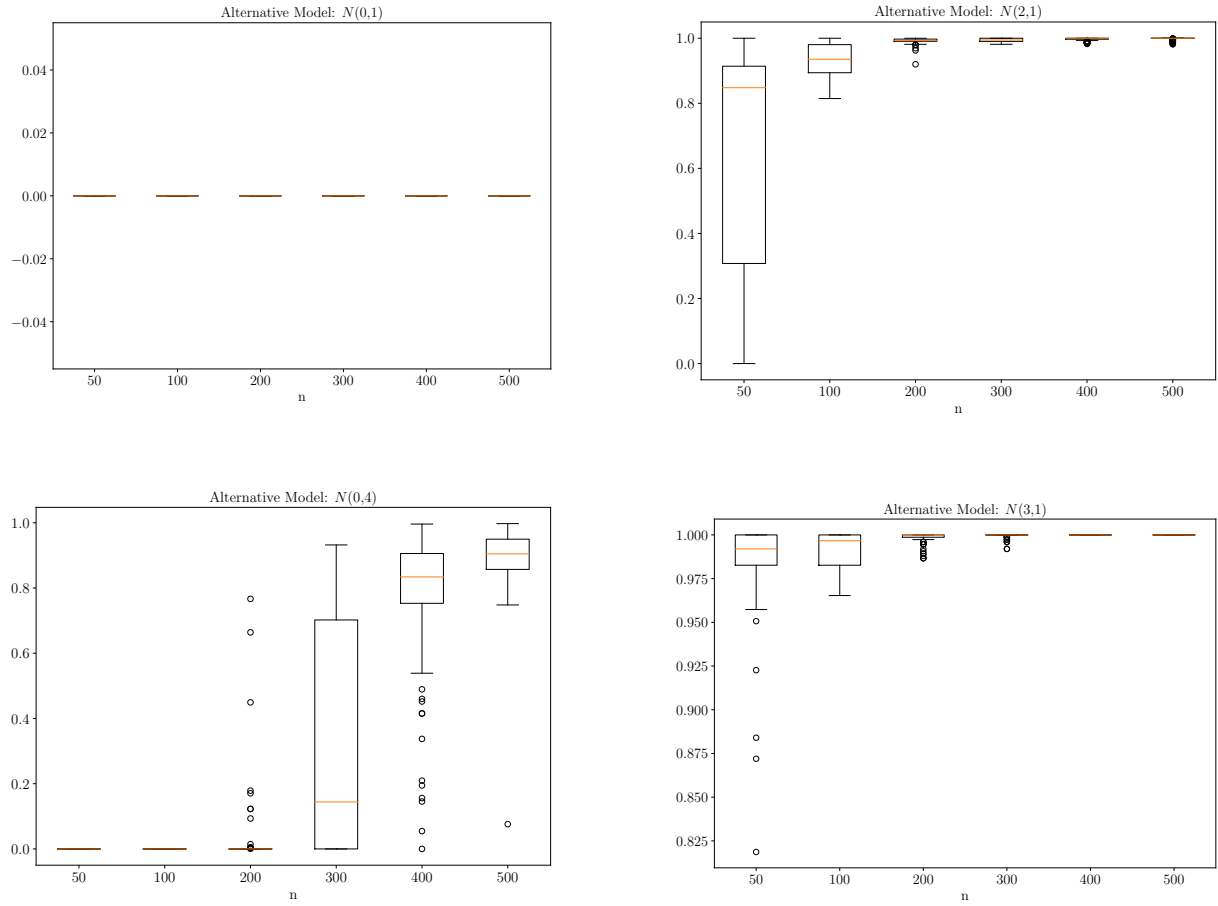


Figure 16: 1-dimensional Gaussian experiment: distribution (over 100 independent runs) of the probability of the alternative hypothesis $p(M = 1|\mathcal{D})$ for a different number of observations n . The null hypothesis is both samples X and Y are i.i.d. $\mathcal{N}(0, 1)$ (Top Left) and the alternative hypothesis is $Y \stackrel{i.i.d.}{\sim} \mathcal{N}(2, 1)$ (Top Right), $Y \stackrel{i.i.d.}{\sim} \mathcal{N}(0, 4)$ (Bottom Left) and $Y \stackrel{i.i.d.}{\sim} \mathcal{N}(3, 1)$ (Bottom Right). As expected, the proposed method is able to detect the difference between the given samples.

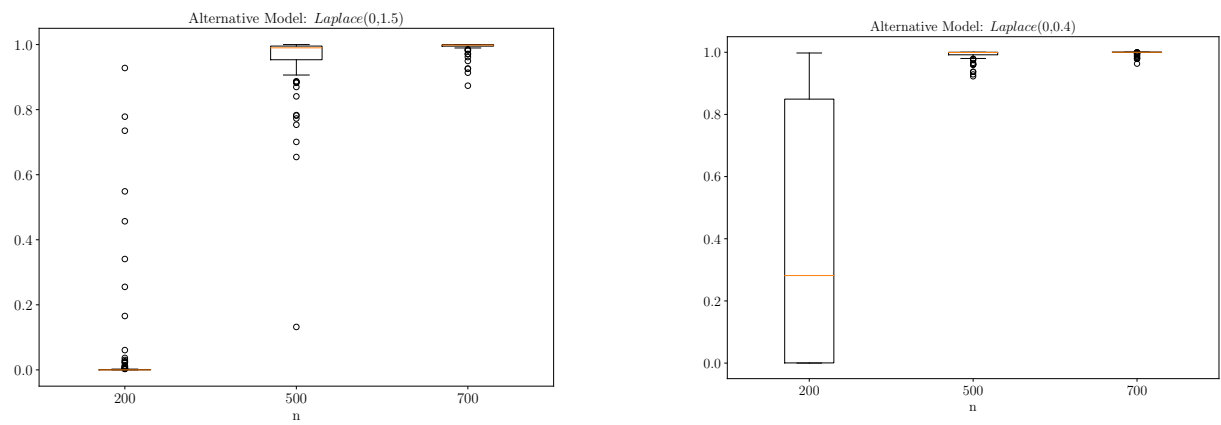


Figure 17: 1-dimensional experiment comparing correlated Gaussian and Laplace distributions: distribution (over 100 independent runs) of the probability of the alternative hypothesis $M = 1 | \mathcal{D}$ for a different number of samples n . (Left) $X \stackrel{i.i.d.}{\sim} \mathcal{N}(0, 1)$ and $Y \stackrel{i.i.d.}{\sim} \text{Laplace}(0, 1.5)$. (Right) $X \stackrel{i.i.d.}{\sim} \mathcal{N}(0, 1)$ and $Y \stackrel{i.i.d.}{\sim} \text{Laplace}(0, 0.4)$. The random variables X and Y are correlated with correlation 0.5.

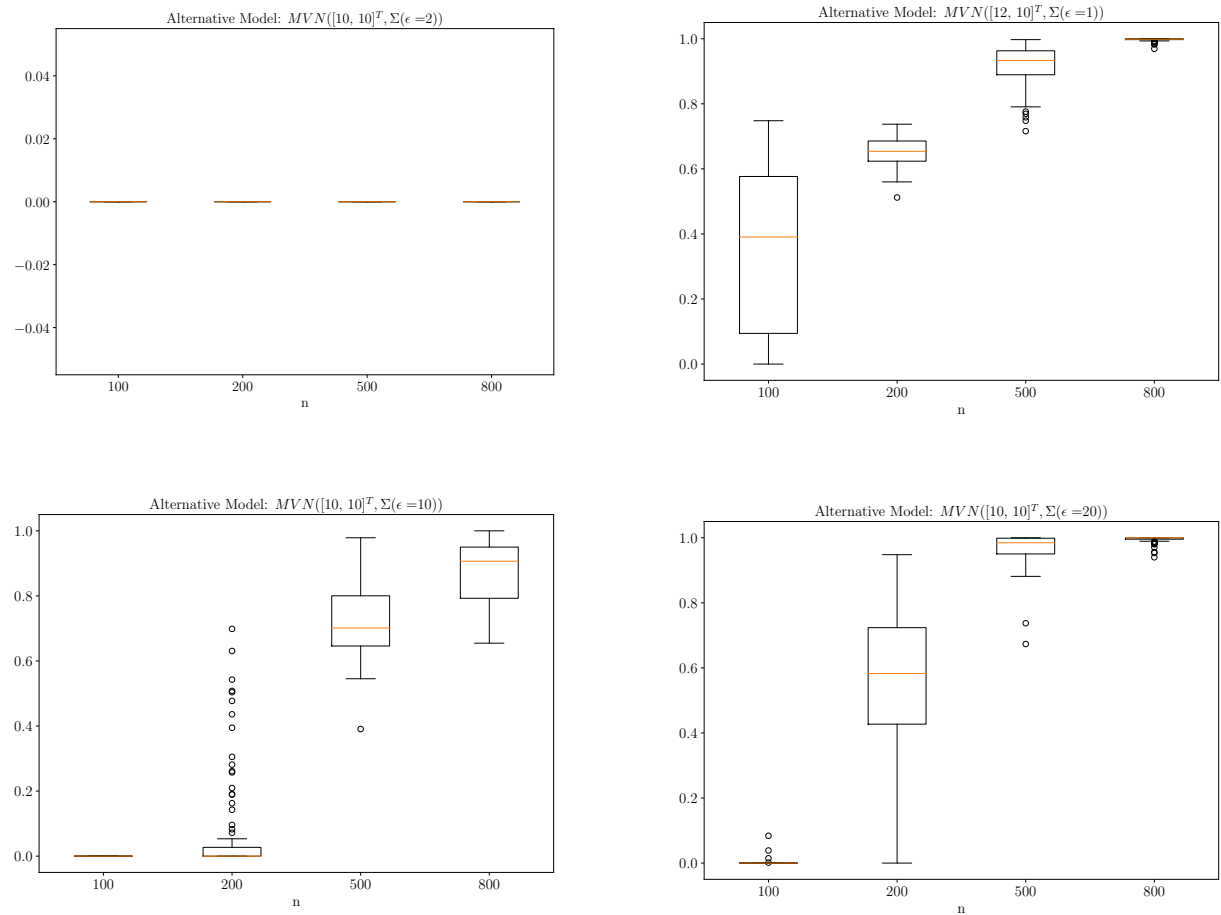


Figure 18: 2-dimensional Gaussian experiment: distribution (over 100 independent runs) of the probability of the alternative hypothesis $p(M = 1 | \mathcal{D})$ for a different number of observations n . The null hypothesis is that both random variables follows a bivariate Gaussian distribution centered at $[10, 10]^T$ with identity covariance matrix. Under the alternative hypothesis, the distribution of Y stated on top of each plot.

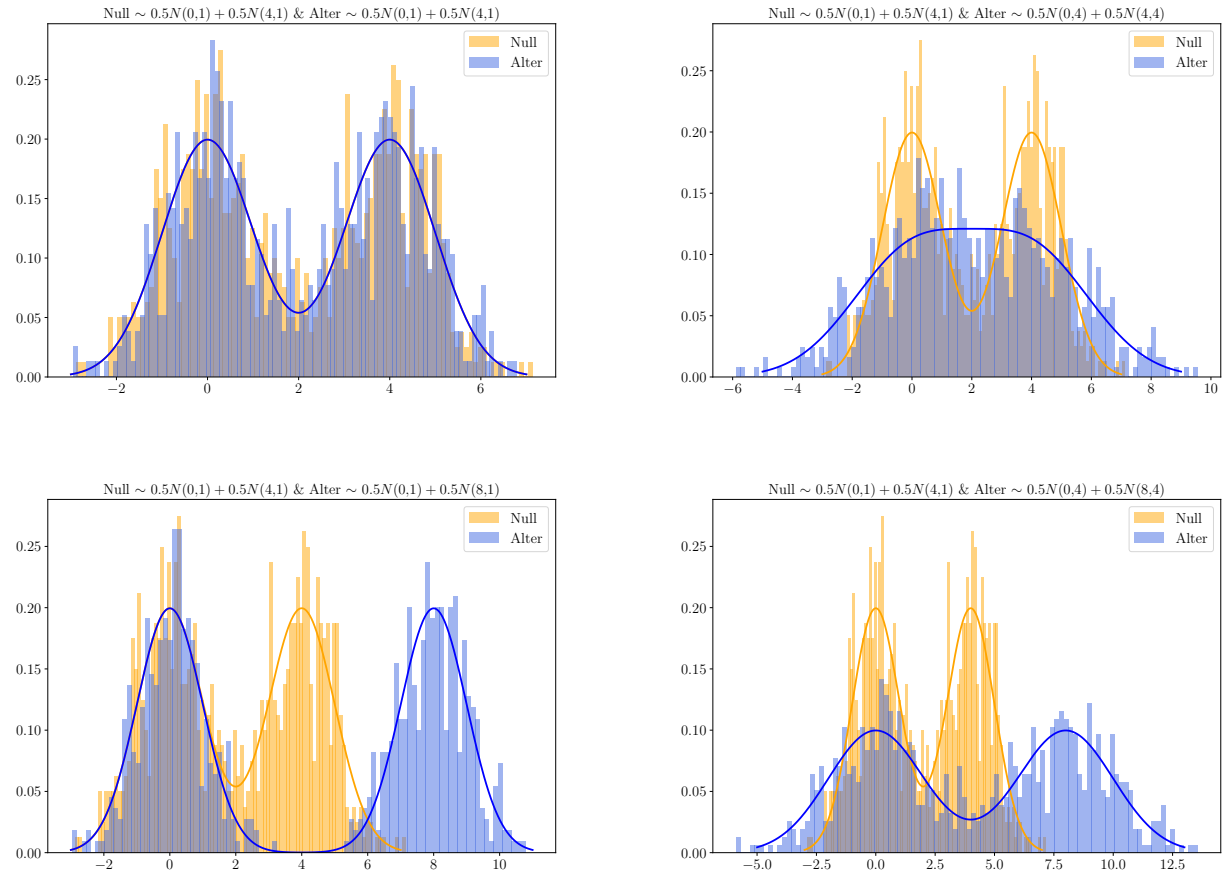


Figure 19: Visualisation of 1-dimensional mixture of Gaussian distributions from Section 9 with 800 samples each. Continue onto the next page.

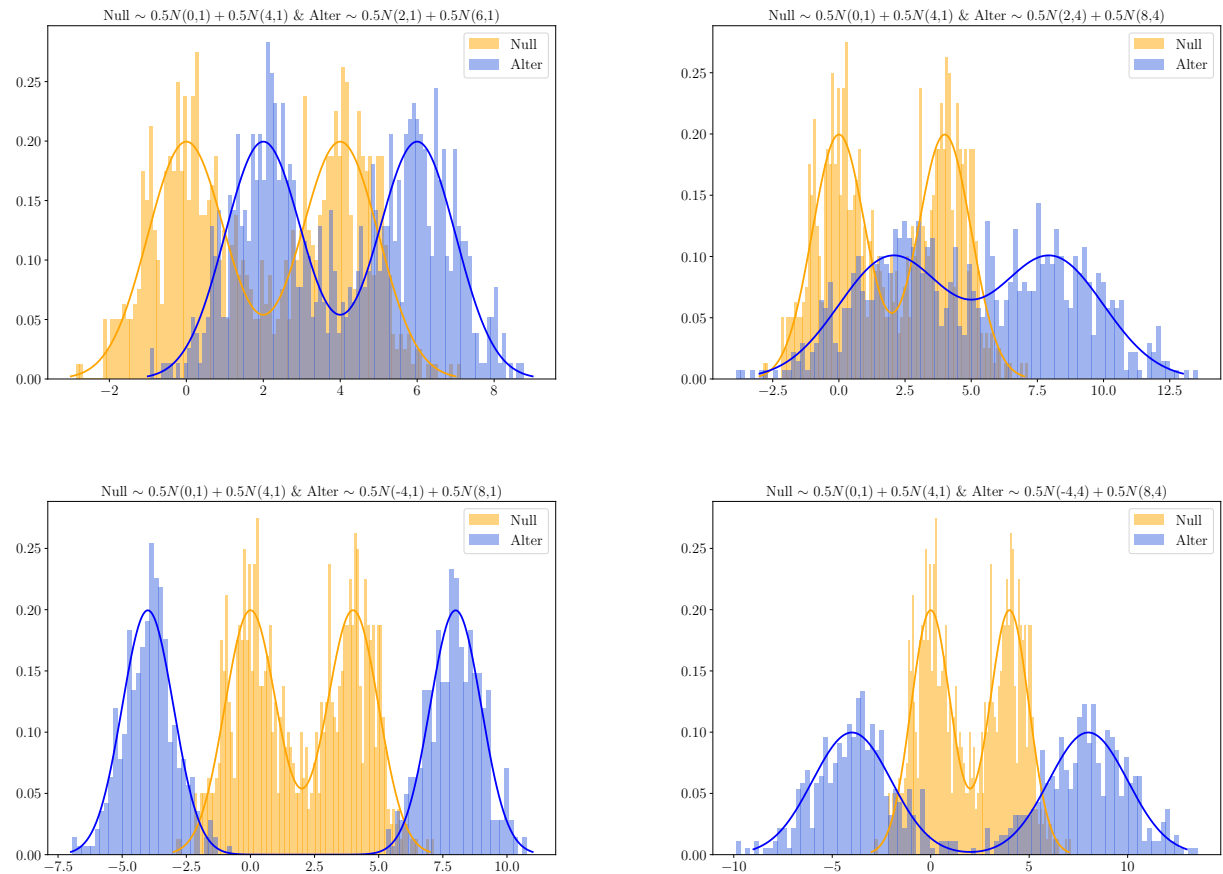


Figure 20: Visualisation of 1-dimensional mixture of Gaussian distributions from Section 9 with 800 samples each.

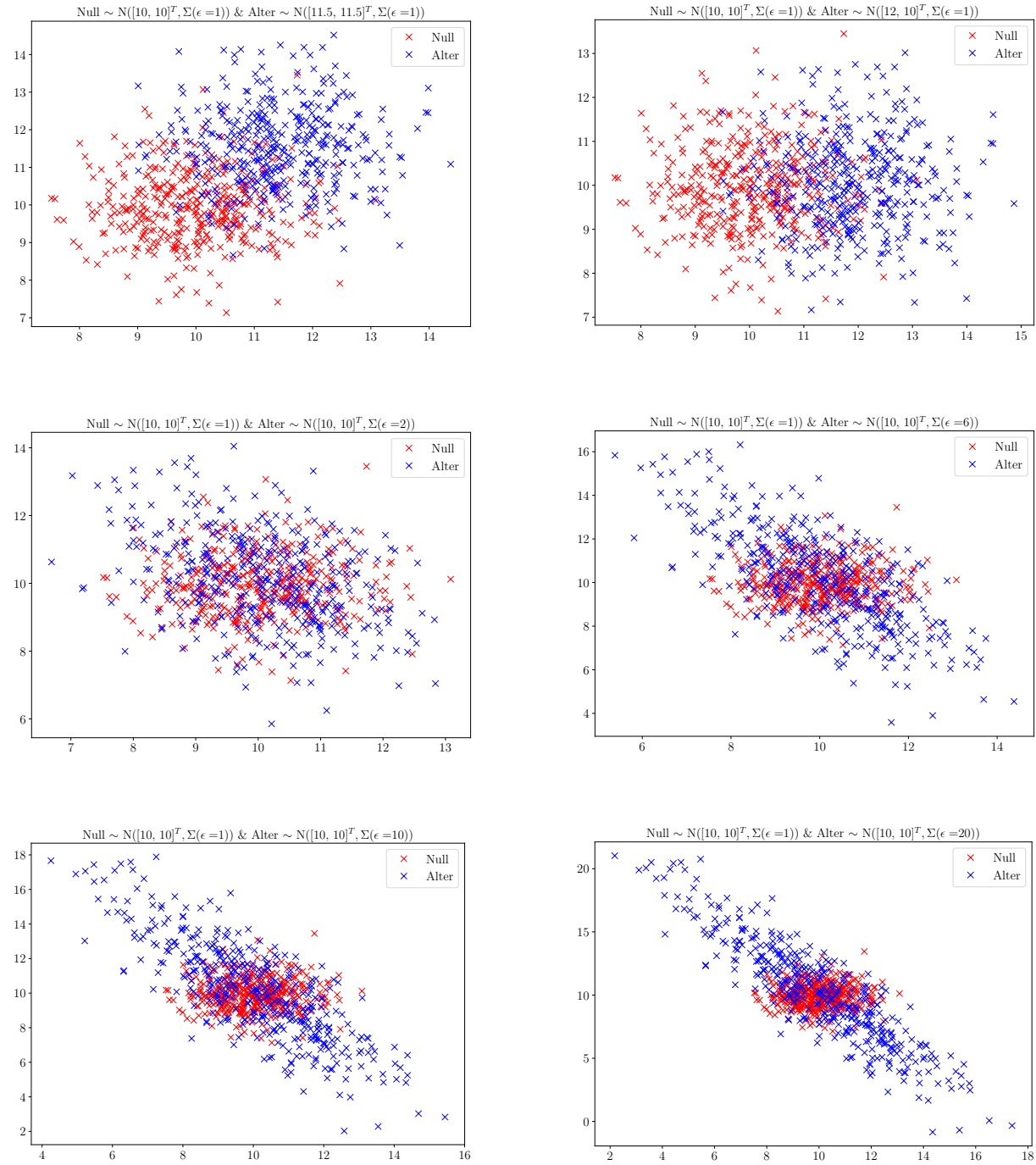


Figure 21: Visualisation of 2-dimensional Gaussian distributions discussed in the main text with 400 samples each.

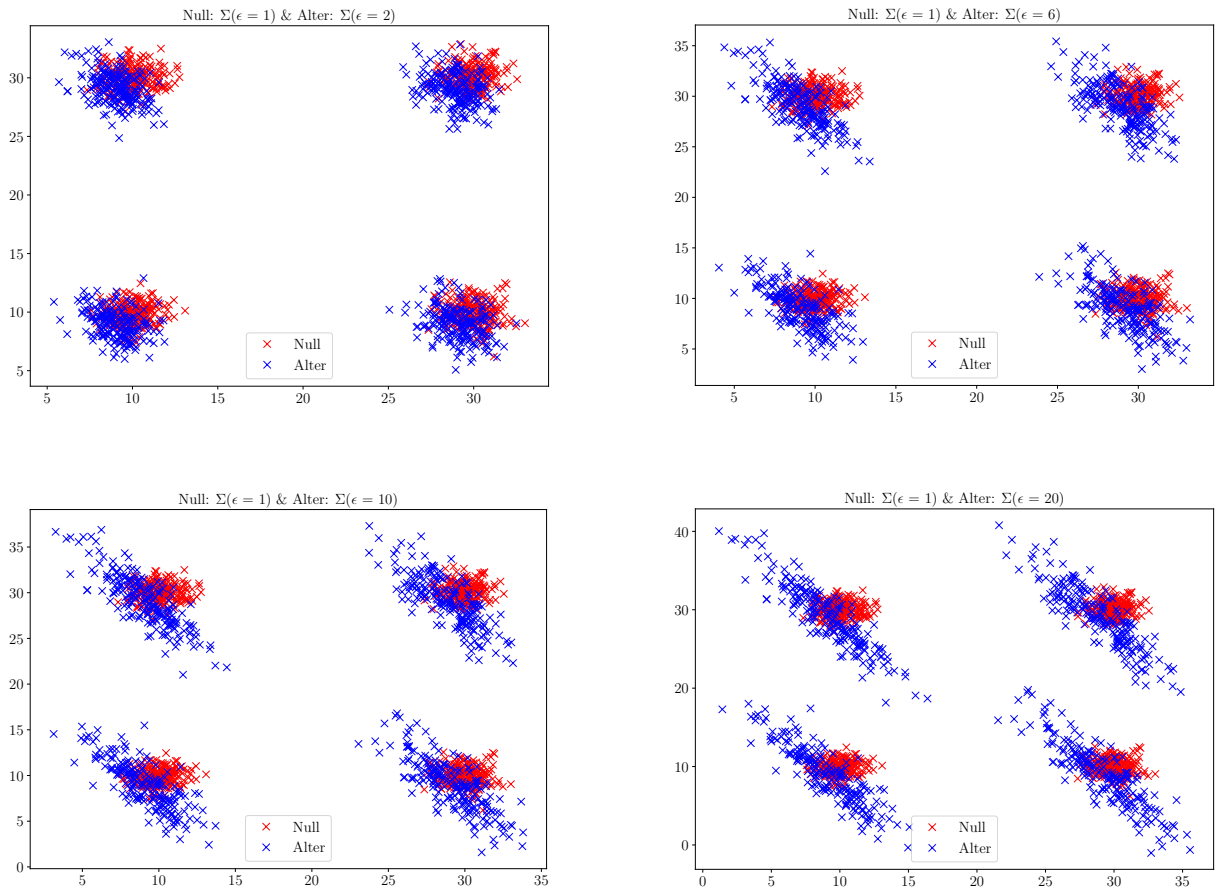


Figure 22: Visualisation of 2 by 2 Blobs of 2-dimensional Gaussian distributions discussed in the main text with 200 samples in each blob.